

Final Report

Project Title: **Measurement Method and Causes Analysis of Curl in Newsprint**

Project Number: AiF-No. 14169 N
Duration: 01.07.2004 – 30.06.2006

Principle Investigators:

Mr. S. Zhao, PMV
Ms. M. Niedernhuber PMV

Project Team:

Mr. M. Albrecht UPM-Kymmene GmbH & Co. KG
Dr. C. Bülow ehemals: Julius Schulte Söhne GmbH & Co.
Mr. J. Kracke Papier- und Kartonfabrik Varel GmbH & Co. KG
Ms. F. Schütt Stora Enso Sachsen GmbH
Mr. C. Schut Papierfabrik Heil GmbH
Dr. D. Rhodius Papierfabrik Schoellershammer GmbH & Co. KG
Mr. J. Ullmann Kübler & Niethammer
Dr. J. A. Wiedmann Buchmann GmbH Kartonfabrik
Mr. M. Dinkel Lang GmbH Papierfabrik

1 Abstract

Contents

1	Abstract.....	2
2	Introduction.....	7
2.1	Definition of curl in paper.....	7
2.2	Origins of curl.....	8
2.3	Geometrical types of curl.....	9
2.4	Available curl measurement methods.....	10
2.5	Goals of the project.....	12
3	State of the art.....	13
3.1	Previous research.....	13
3.1.1	Curl.....	13
3.1.2	Fibre orientation.....	17
3.1.2.1	Orientation in the paper sheet.....	17
3.1.2.2	Fibre orientation across sheet thickness.....	18
4	The new curl measurement method.....	20
4.1	Curl measurement system.....	20
4.1.1	System setup (hardware).....	21
4.1.2	Software packages.....	21
4.1.3	Measurement procedures.....	23
4.2	Climate chamber for sample treatment.....	23
4.3	Operation of the imaging system.....	24
4.3.1	Principle of coded light procedure.....	25
4.3.2	Application of the coded light method for curl measurement.....	26
4.3.3	Calibration of the imaging system.....	27
4.4	Sample preparation.....	28
4.4.1	H-shape die-cutting.....	29
4.4.2	Star-shape die-cutting.....	29
4.5	Treatment of the paper sample.....	31
4.6	Architecture of the curl measurement method.....	32
4.7	Data pre-processing.....	33
4.8	Identification of the height and the curvature of the curl.....	34
4.8.1	Curl height.....	34
4.8.2	Curvature of curl.....	35
4.8.2.1	Direct evaluation method.....	35
4.8.2.2	Indirect evaluation method.....	37
4.9	Dynamic curl.....	38

5	Experimental work.....	39
5.1	Laboratory sheets	39
5.1.1	Fibre properties.....	40
5.2	Industrial paper samples.....	40
5.3	Measurement methods.....	41
5.3.1	Hygroexpansion.....	41
5.3.2	Fibre orientation	41
5.3.3	Effect of reaction time on curl.....	42
6	Results and discussions.....	43
6.1	Verification of the new measurement method.....	43
6.2	Relationship between curvature and curl height.....	44
6.3	Effect of fibre orientation on the curl in paper	44
6.4	Effect of hygroexpansion on the curl in paper.....	46
6.5	Influence of basis weight on the curl in paper.....	46
6.6	Effect of cyclical humidity change on the curl in paper	47
6.7	Curl in newsprint.....	48
6.8	Measurement of dynamic curl.....	50
7	Literature Cited.....	52
8	Appendix A – Curl measurement results	56
9	Appendix B – Drawings of the climate chamber	59
10	Appendix C – GUI of the Curl Analysis Program	62
11	Appendix D – Source Codes.....	63
11.1	Calibration program	63
11.2	Measurement program.....	67
11.3	Analysis program	72

List of Figures

Figure 1: Classification of different types of curl in paper.....	9
Figure 2: Curl measured in inches.....	10
Figure 3: Curl measured in degrees.....	11
Figure 4: Plate scales.....	11
Figure 5: Cross cut.....	11
Figure 6: The various forms of out-of-plane deformations.....	14
Figure 7: Device for simulating and measuring the curl.....	16
Figure 8: Tiger stripes – fibre orientation streaks.....	18
Figure 9: Model of the origin of the fiber alignment.....	19
Figure 10: The curl measurement and analysis system.....	20
Figure 11: Program flow chart of the calibration of the image system and measurement of curl in a sample ...	22
Figure 12: Program flow chart of the curl analysis software.....	22
Figure 13: Schematic diagram of the climate chamber[48].....	24
Figure 14: The coded light principle.....	25
Figure 15: Line patterns generated by the line projector.....	26
Figure 16: Setup of the curl detecting system.....	27
Figure 17: The 2-D (left) and 3-D (right) images of the curl formed on strips with a typical H-shape cut.....	29
Figure 18: The star-shape die-cutting template.....	30
Figure 19: Typical curls in a paper sample die-cut in star shape.....	30
Figure 20: Bending curvature response to cyclical humidity changes when the process starts from the desorption stage.....	31
Figure 21: Bending curvature response to cyclical humidity changes when the process starts from the adsorption stage.....	32
Figure 22: Curl measurement and analysis architecture.....	33
Figure 23: Height and curvature of a curl.....	35
Figure 24: Circle fitting with direct evaluation method.....	37
Figure 25: Curvature calculation – second method.....	38
Figure 26: The influence of basis weight on the curl response of paper at 95% RH.....	42
Figure 27: Curl of photobase papers.....	43
Figure 28: Curvature vs. curl height.....	44
Figure 29: Effect of duplex sheets.....	45
Figure 30: Influence of fibre orientation on curl.....	45
Figure 31: Effect of hygroexpansion on curl.....	46
Figure 32: Influence of grammage (basis weight) on curl.....	47
Figure 33: Curl und cyclical humidity change.....	48
Figure 34: CD profile of curl in newsprint.....	49
Figure 35: CD profile of TSO angle in newsprint.....	49

Figure 36: CD profile of TSI MD/CD ratio in newsprint	50
Figure 37: Dynamic curl in paper of basis weight 45 g/m ²	51

2 Introduction

Paper is a hygroscopic porous material. It expands or contracts due to changes in moisture content. Mathematically, paper can be considered as multi-layered structure [1, 2]. If the physical properties of each “layer” differ from one another or there are moisture content gradient along paper thickness direction, the hygroexpansions of each “layers” vary in the corresponding manner. Consequently, the out-of-plane deformation (curl) appears.

Curl in paper is a long-standing problem since the departure from the flat may seriously affect the processing of paper [3-6]. Excessive curl reduces the quality of paper, and it affects the customers as it is the most common cause for sheet feeding problems. For this reason, customers impose strict limits on the curl and hence it is becoming increasingly important to produce a paper with a limited curl.

Curl occurs in almost all paper and board grades, but it causes most problems when printing or copying of paper sheets. The appearance of curly sheets is not satisfactory. In printing papers, curl may cause “rolling” of the front pages of a newspaper or magazine that contains four-color printing while the opposite side is black and white [7].

The stringent international market requirements demand for high paper quality preferably “curl-free”. To meet the quality requirements, curl in paper must be measured instantly close to the producing line. Unfortunately there is no fast, uncomplicated, yet accurate measurement method available today for characterizing curl in paper. Furthermore the factors that influence this paper property are not sufficiently clarified.

2.1 Definition of curl in paper

Curl is a type of dimensional instability phenomenon of paper. It is the tendency of paper to depart from a flat form [8, 9]. A TAPPI Technical Information Sheet defines curl as “The tendency of unrestrained flat paper sheets to distort and form curved surfaces of essentially cylindrical shape” [10].

Although the basic cause of curl is simply a differential deformation of paper in its thickness direction, i.e., the in-plane deformation, varies in the thickness direction, the processes causing the differential deformation are complex and variable.

2.2 *Origins of curl*

During the paper manufacturing process, a well-dispersed fibre suspension with a minimum of flocks and a uniform and stable jet across the width of the machine without lateral velocities, random components, or streaks should be produced by the headbox. The fibre suspension is further delivered to the wire section where the drainage of water occurs and wet web is formed.

The wet web is then conveyed to press section to remove the remaining water as much as possible before drying because drying is the most expensive means to remove water from paper during the papermaking process. Since water in paper cannot be removed completely with mechanical treatment only, dryers usually consisting of many large steam-heated cylinders are employed to make the paper reach the target dryness.

To improve the optical and mechanical properties and to produce “homogeneous” sheet, fillers and chemicals (retention, drainage and formation aids) are often dosed in the fibre suspension before it enters the headbox.

Fibers become preferentially oriented in the machine direction during passage through a tapered headbox [11]. The fibre orientation is further enhanced by big jet-to-wire ratio. When the slice jet lands on the forming wire, the bottom of the jet which contacts the wire forms the mat first due to dewater by water remove elements underneath the wire and nature drainage caused by gravity on a horizontally aligned single-wire former (On a twin-wire or gap former, the dewatering process happens simultaneously on both sides of the jet). Before all the fibres in the suspension are immobilized, they can change their orientation to a different angle than the fibres already deposited/tangled on the mat. Therefore, fibre orientation in different “layers” in a paper may vary from layer to layer. This is an important factor that affects curl [4, 12-15].

Due to the suction of dewatering elements and filtration effect of the first formed mat, the layer in a paper close to forming wire (bottom side) has lower contents of fillers and fibre fines than the inner layers, and the top side has the highest contents. The uneven distribution of fillers and fines in paper is another factor affecting curl.

There are many other factors that can affect curl. For example, paper density two-sidedness, asymmetrical drying and one side coating, etc. In general, any structural variations through paper thickness direction and papermaking processes that can deeply influence the paper properties such as fibre orientation, density and hygroexpansion can affect curl in paper.

2.3 Geometrical types of curl

There are various types of curl that can be observed in paper. Based on the shape and the principle axis of the curl, it can be defined as CD (cross-machine direction), MD (machine direction) and diagonal curl as shown in Figure 1. If the curl axis is along the MD direction of paper, it is called CD curl. Similarly, MD curl has axis along CD direction, and diagonal curl along diagonal direction. Dependent on the side of the curvature (concave side), each form is further classified as top side or bottom side curl.

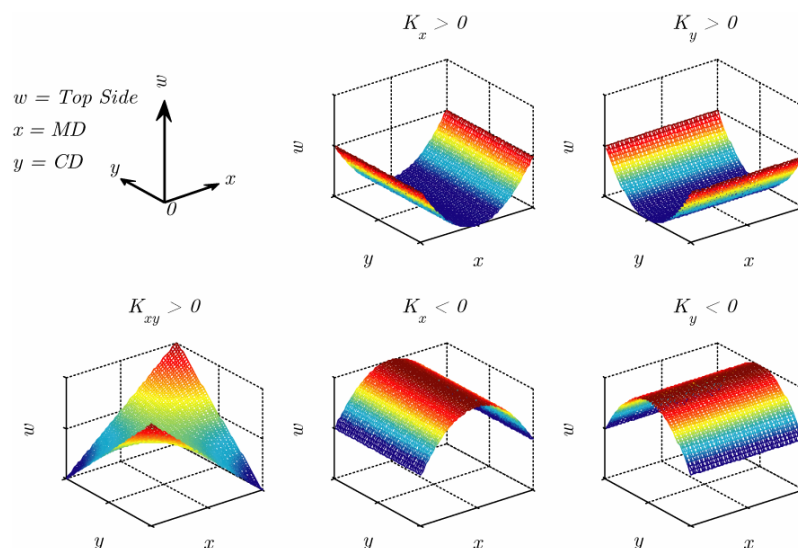


Figure 1: Classification of different types of curl in paper

Mathematically, the curl in paper can be described by three components K_x , K_y and K_{xy} which correspond to MD, CD and diagonal curvatures respectively. These curvatures are defined as,

$$\begin{aligned}
 K_x &= K_{MD} = \frac{\|w\|^2}{\|x\|^2}, \\
 K_y &= K_{CD} = \frac{\|w\|^2}{\|y\|^2}, \\
 K_{xy} &= K_{TW} + 2 \frac{\|w\|^2}{\|x\|\|y\|},
 \end{aligned} \tag{1}$$

where K_{TW} is the twist curl component. Consequently, the out-of-plane deviation of the sheet, w , can be defined as,

$$w(x,y) = \frac{1}{2}K_x x^2 + \frac{1}{2}K_y y^2 + \frac{1}{2}K_{xy}xy + a + bx + cy \tag{2}$$

The last three terms, $a + bx + cy$, are included for completeness. They account for any displacement or tilting of the specimen relative to the origin of the xy -plane[16]. The physical meanings of K_x , K_y are the reciprocals of the radii of MD and CD curl, respectively, i.e.,

$$K_x = \frac{1}{R_x}, \text{ and } K_y = \frac{1}{R_y}.$$

Figure 1 shows several types of curl that are possible in a paper sheet, namely, MD top side curl ($K_x > 0$), CD top side curl ($K_y > 0$), MD bottom side curl ($K_x < 0$), CD bottom side curl ($K_y < 0$), and diagonal curl ($K_{xy} > 0$).

2.4 Available curl measurement methods

There are not any current curl measurement methods which would be applicable to most situations of curl which occur in practice. Paper manufactures, paper consumers, and research institutes usually have their own methods for measuring the curl. Langevin and Giguere [17] reviewed several manufacture's methods (Figure 2 – 5).



Figure 2: Curl measured in inches

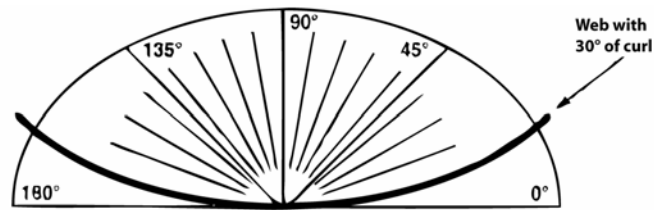


Figure 3: Curl measured in degrees

Some papermakers and converters use a scale or protractor to measure curl in millimetres or degrees (Figure 2, 3). To use these methods, paper samples are cut into a specific size and placed into climate chambers with varying humidities at 20 % RH, 50 % RH and 70 % RH. The samples are allowed to condition for approximately half an hour before they are removed from the chambers. A scale or a protractor is placed next to each sample, the corresponding “inches of curl” or “degrees of curl” are recorded.



Figure 4: Plate scales

Some papermakers use a set of plates (Figure 4) representing a variety of common paper curl shapes. A technician uses these plates by cutting samples of the paper produced and placing the sample next to the plate that most closely approximates the shape the paper has taken. Certain plates represent acceptable curl behaviour, while others represent unacceptable behaviour.

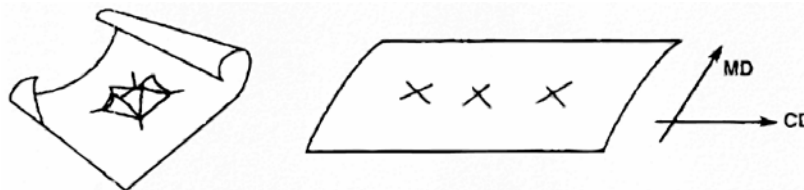


Figure 5: Cross cut

Another very popular curl measurement method is the “Cross cut” (Figure 5). In this method, a sample of size 250 mm × 250 mm or 300 mm × 600 mm is cut from the manufactured product. A cross is then cut in various locations on the sample, and then the sheet is inspected for both MD and CD curl.

There are other curl measurement methods available, for example, the DIN 66 018 method for the determination of the curvature of carton board. However, there is no fast and easy method for the measurement of curl available today.

2.5 Goals of the project

Since there is no generally recognized measuring instrument for the measurement of curl, the main target of this research project is the development of a curl analyzer based on image analysis techniques.

It is widely recognized that fibre orientation has direct effect on the curl. After the development of the curl analyzer, the effect of fibre orientation on the curl is to be examined both with laboratory made sheets and machine papers.

The goal of the research project is divided into the following sections:

1. Development of a suitable measuring procedure for the characterization of curl.
2. Investigation of the influence of fibre orientation on the curl at laboratory papers.
3. Investigation of the influence of hygroexpansion, fibre orientation, surface-related mass and transverse shrinkage on the curl.
4. Correlation of curvature with suspension, paper and paper-making machine data.

For the execution of this project, paper specimens from different newsprint paper machines were requested and examined.

3 State of the art

In addition to the measurement methods available for characterizing curl in paper which have been discussed in Chapter 2.4, there are still other measurement devices on the market to measure curl in paper. The Finish company Ambertec Oy offers an off-line measuring instrument (Surface Orientation Tester) and ABB offers an on-line sensor – the Smart Fibre Orientation Sensor – for measuring the two-sidedness of the fibre orientation within paper.

So far, however, there is no generally accepted curl measuring device. Therefore, the research project is to develop a curl measurement instrument, consequently the factors which have influences on curl can be examined. It is known that the two-sidedness of fibre orientation and hygroexpansion affects the curl; however, there are no quantitative correlations between them so far. Moreover, it is not well-known of the effect of the paper machine variables, furnish composition, as well as the cross-machine direction (CD) basis weight profile and the CD shrinkage profile of the paper web on the curl behaviour of paper.

3.1 Previous research

3.1.1 Curl

Out-of-plane deformation shows up if the surface of the paper or carton board deviates from a mathematically even surface within a macro scale. This deformation can be in the form of curl, wavy edges, tight edges, cockling or wrinkle [18] (Figure 6).

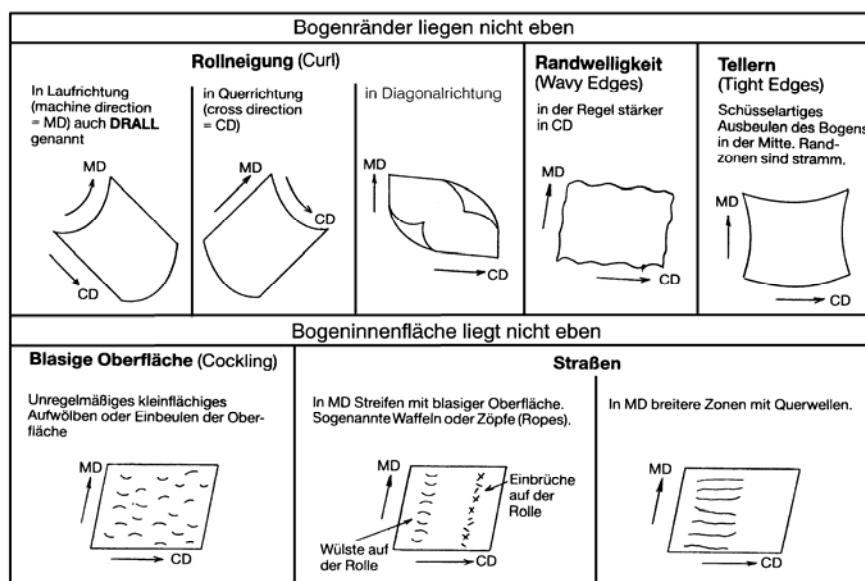


Figure 6: The various forms of out-of-plane deformations

As been discussed previously, the curl in paper can take place in papermachine direction (MD), cross-machine direction (CD) or diagonal direction. It may be caused [7]:

1. by the production process on the paper machine;
2. as reaction to a change of the moisture content of paper;
3. by one-sided printing, coating or copying process (copy paper).

Therefore a pronounced curl limits both the workability and application type of a paper strongly.

In the literature, the causes for curl in paper were attributed to the structural variations on the cross direction of the paper sheet. The fundamental structural variation studied was fibre orientation. Other structural variations such as content of fillers and fines, density variations, frozen tensions during the paper drying process which become relaxed when re-moisturised, were also discussed. The curl tendency of paper is influenced by papermaking process from the headbox, the former, the press section to the dryer section. In addition, it is also influenced by different surface treatments for instance, sizing, coating and lamination [7, 19-26]. Paper produced on a hybrid former is more instable than that on roll-blade former [27]. Furthermore it is well-known that the curl is strengthened with increasing beating degree and hygroexpansivity as well as decreasing thickness of paper, accordingly increase the content of short fibres and addition of waxy or moisture retentive substances like Sorbitol were

suggested as the counter measures for curl [18, 21]. Geenen [18] also proposed several measures to tackle the curl problem. Since the stiffness of paper prevents curl, it is understandable that the curl in paper caused by different moisture contents in the surrounding air is the strongest in sheets made of softwood pulp, followed by semi-chemical pulp and groundwood. A high content of filler also yields instability [21, 28, 29].

Theoretical considerations by Carlsson [2], who regards paper as a laminate, show that curl depends mainly on the different coefficients of expansion of both sides of the sheet during moisture absorption, and the shape of the curl is determined by the fibre orientation angle due to anisotropy [2, 30]. With the inclusion of nonlinear elements the rigidity influences are considered as frozen tensions in the mathematical model. And the curl can be modelled by finite elements method [20, 31].

If the two sides of paper are dried rapidly and unevenly, the paper always curls concavely to the side been dried last [21]. Since paper dimension usually changes more strongly in CD than in MD, a CD curl prevails predominantly. It can experimentally be shown that rewetted and dried strips of newsprint and uncoated paper, which are cut in machine direction have a right-handed curl, while the strips cut in CD direction exhibit a left-handed curl [32]. Furthermore, the curl depends on the size of the strips. The curl behaviour of a strip is usually different from that of a sheet. Fibre orientation is responsible for the twist curl in corrugated board base paper, the diagonal curl in copying paper and the lack of piling stability in writing paper [33].

For the examination of the curl different procedures are available. The cross cut method is the simplest, with which a cross is cut on the paper web in several places. Curl can be detected from the deformations at the cutting sites [17].

According to the withdrawn Tappi method T 466 cm-82 the single-sided humidification is employed. The curl indicator shows the time it takes to reach the maximum curl or the height of the curvature.

The magnitude of curl can also be measured with a sample size from 150 mm × 150 mm to 200 mm × 200 mm after 30 minutes conditioned in a climate chamber with 20 %, 50 % or 70 % relative humidity. Based on the similar principle the curvature of carton board can be measured according to DIN 66 018 standard.

For the inspection of curl Brecht used a special test apparatus. It consists of a plexiglass cabinet, which has a square opening on the top cover plate where the sample is placed (see Figure 7).

With salt or sulphuric acid solutions different relative air humidities can be generated in the space above the solution and beneath the paper sample, while the climate (temperature, relative humidity) above the sample keeps constant at lower humidity than that inside the cabinet. Therefore the fibers on the bottom side of the sample surface swell more strongly than those on the top side, which leads to the curl in the paper sample after certain time. The height of the curl is measured in millimetres [28].

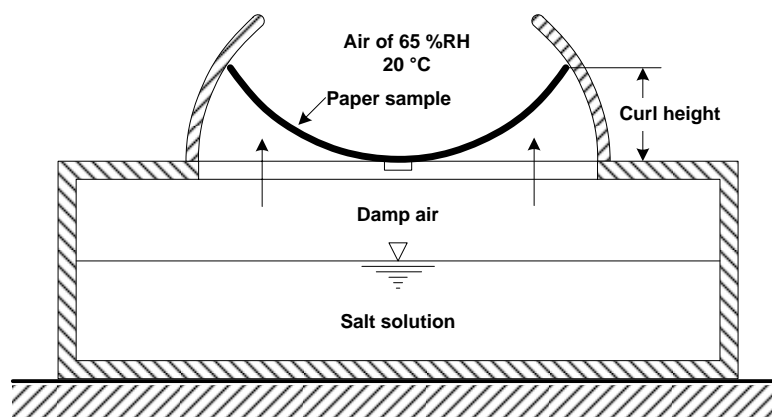


Figure 7: Device for simulating and measuring the curl

The Finish research institute for pulp and paper industry KCL (Oy Keskuslaboratorio – Centrallaboratorium AB) located in Helsinki has developed an optical system named as “Opticum-2”. By changing the relative humidity between 5 % and 85 %, the curl (CD, MD, and diagonal direction) formed in a 90 mm round paper sample can be detected by an optical distance sensor [34].

Another curl meter works on vertically hung up square samples, which curvature is measured by a laser sensor from point to point. With the vertical arrangement of the samples the influence of the force of gravity is negligible and the measurement error for paper of grammage 40 g/m^2 is only about 4 % [35].

According to Viitaharju, Kajanto and Niskanen [34] the curl of wood-containing paper can also be characterized by put a stack of 10 sheets into an oven for 10 min at 103 °C and measuring the upward displacement of the edges of the upper sheet immediately after the drying process.

3.1.2 Fibre orientation

The length of fibre is 100 times bigger than its width. When a fibre deposits onto the wire, it aligns more or less to the machine direction according to the jet-wire velocity difference. It may also align to different directions in layers through thickness direction.

3.1.2.1 Orientation in the paper sheet

If a sheet is made from fibre suspension on a laboratory sheet former, statistically the fibres in the sheet are distributed evenly in all directions consequently the sheet is isotropic. By contrast, machine made paper exhibits anisotropy in regarding fibre orientation. The angle deviation of the fibre orientation direction to machine direction is called fibre orientation angle. It can be analysed by measuring of coloured fibres, which are added to the suspension before sheet forming.

Usually the anisotropy of fibre distribution can be calculated by the ratio of the fibre orientation frequency in MD to that in CD [36-38]. The ratio of zero span breaking length in MD and CD direction gives an indication of the fibre orientation anisotropy and the strength of the fibre orientation [39].

For the determination of fibre orientation there are different measuring instruments, which are based on different measuring procedures. Fibre orientation can be measured by means of microwaves (energy absorption), ultrasonic (sound propagation), X-ray (diffraction) or scattering of laser light.

The causes for the development of the fibre orientations are mainly in the headbox with recirculation to produce turbulence and the wire as well as the drainage elements in the wire

section (the arrangement of forming boards and forming rolls) [36, 37, 40, 41]. If the jet of stock leaves the headbox with a small angle α_{jet} to machine running direction, there is a relative velocity v_{rel} resulting from the vector addition of jet and wire speed vectors. Fibre orientation takes place mainly along the relative velocity, from which a fibre orientation angle β results. Even with small jet angle deviations substantial fibre orientation angles can develop. During the transition of jet-wire velocity difference from positive to negative, the longitudinal component of the relative velocity ($v_{jet} - v_{wire}$) becomes negative. Therefore the fibre orientation angle changes the sign [19].

From recent investigations we know that the flow conditions in the headbox can lead to the fact that fibres within lamellae range from approximately 1 to 3 cm broad exhibit a strong longitudinal orientation, which is the case for paper surface layer(s). In machine running direction lightweight papers can have running waves, a feature which is sometimes designated as cockling. With inclined illumination the fibre orientation streaks are shown as gloss places [42-44].

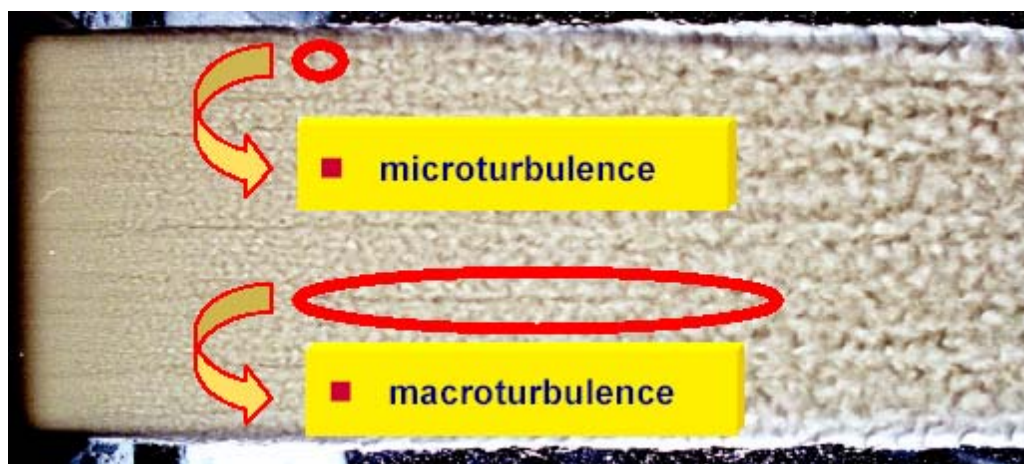


Figure 8: Tiger stripes – fibre orientation streaks

A form of fibre orientation streaks, called “tiger strips”, is caused by extensive microturbulence in the jet from the headbox. It can be diminished by transiting the jet flow from microturbulence to macroturbulence.

3.1.2.2 Fibre orientation across sheet thickness

The magnitude of fibre orientation (anisotropy) is determined decisively by the velocity difference between the jet and the wire. It is the largest at the point of impact of the jet on the endless wire and decreases as the consequence of shearing stresses in the course of the filtration process. Figure 9 shows the situation of the positive jet-wire velocity difference on a Fourdriner wire for the state of laminar flow. At the jet impact point the lower layers of the jet are slowed by the wire. Therefore, the upper layers of the jet move faster than the lower. If there is a fibre perpendicular to the jet direction in the suspension at time t_1 , the top part of the fibre is a big distance forward than the lower part of the fibre at time t_2 in the light of the presence of the relative velocity profile. The fibre turns and is aligned toward the direction of the relative velocity of jet and wire. This process develops further in the drainage course on the wire. For the case of a negative jet-wire velocity difference a similar analysis can be applied.

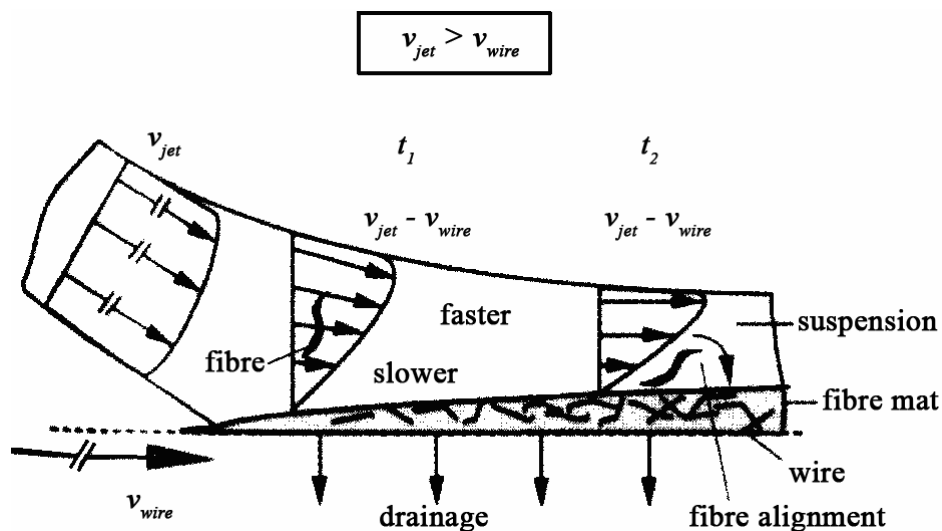


Figure 9: Model of the origin of the fiber alignment

In turbulent flow state the relative velocity profile of the jet is superposed with the three-dimensional fluctuation velocity of the turbulent clusters. The higher the degree of the turbulence and the smaller the relative velocities are, the smaller the fibre-aligning effect is, since the profile of the relative velocities becomes unsteady. As a result of the stated circumstances fibre orientation and anisotropy will vary over the thickness of the sheet. The flow conditions are certainly frozen in paper sheet [19, 45, 46] and can be measured in the individual layers after the sheet splitting.

4 The new curl measurement method

As been discussed previously, a paper specimen can curl in different directions (CD, MD and diagonal) and the curvature may have concave to the top/felt side or bottom/wire side of the paper. To reveal the true curl in paper in these directions, the best way is to cut the paper into narrow strips in the corresponding directions and measure the curls accordingly. To achieve one of the goals of the project – to develop a fast and easy method for curl measurement, the die-cutting of a star shape has been developed. The new curl measurement method based on the image analysis techniques is discussed in this chapter.

4.1 Curl measurement system

The curl measurement system includes both hardware and software packages. In addition, measurement procedures are made to operate the system correctly.

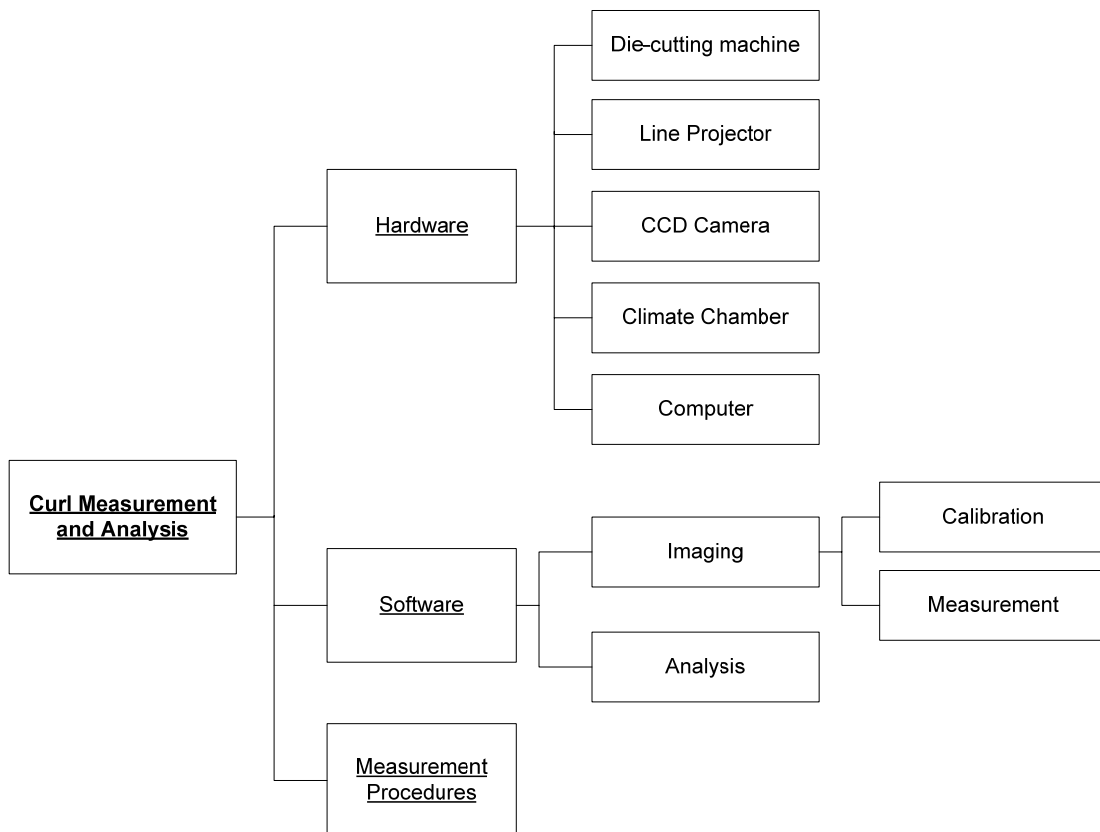


Figure 10: The curl measurement and analysis system

4.1.1 System setup (hardware)

The hardware of curl measurement system consists of a line projector, a digital camera, a climate chamber, a computer with analysis software and a paper sample die-cutting machine.

The line projector is to produce a series of black-and-white line patterns (Figure 15), and casts them onto the surface of the object, in our case, the paper sample at certain angle.

The CCD (charge-coupled device) digital camera captures the line patterns on the paper surface immediately when they are cast by the line projector.

The climate chamber can generate different air humidities to the required levels. The paper sample is conditioned at each humidities for predefined duration of time.

The die-cutting machine cuts a paper sample into H-shape or star-shape for measurement of the curl tendency of the paper. It will be shown later that star-shape prevails over H-shape in several ways.

4.1.2 Software packages

For the measurement and analysis of curl in paper, two software packages were developed. One is for the capturing of a three-dimensional image representing the curled paper sample. The other is for the interpreting of the 3-D image to elicit the curl in a paper sample in the forms of curl height and curvature. Both of them are attached in the appendices.

The imaging system must be calibrated whenever the system has been moved or any device, i.e., the line projector or the camera, has been re-adjusted. After each calibration, the geographical information about the system – the location and position of each device in the system – is stored in a three dimensional map.

The curl analysis software calculates the curl height and estimates the curvature of the curl in a paper sample if there is any curl present. It requires minor user interactions through the graphical user interface.

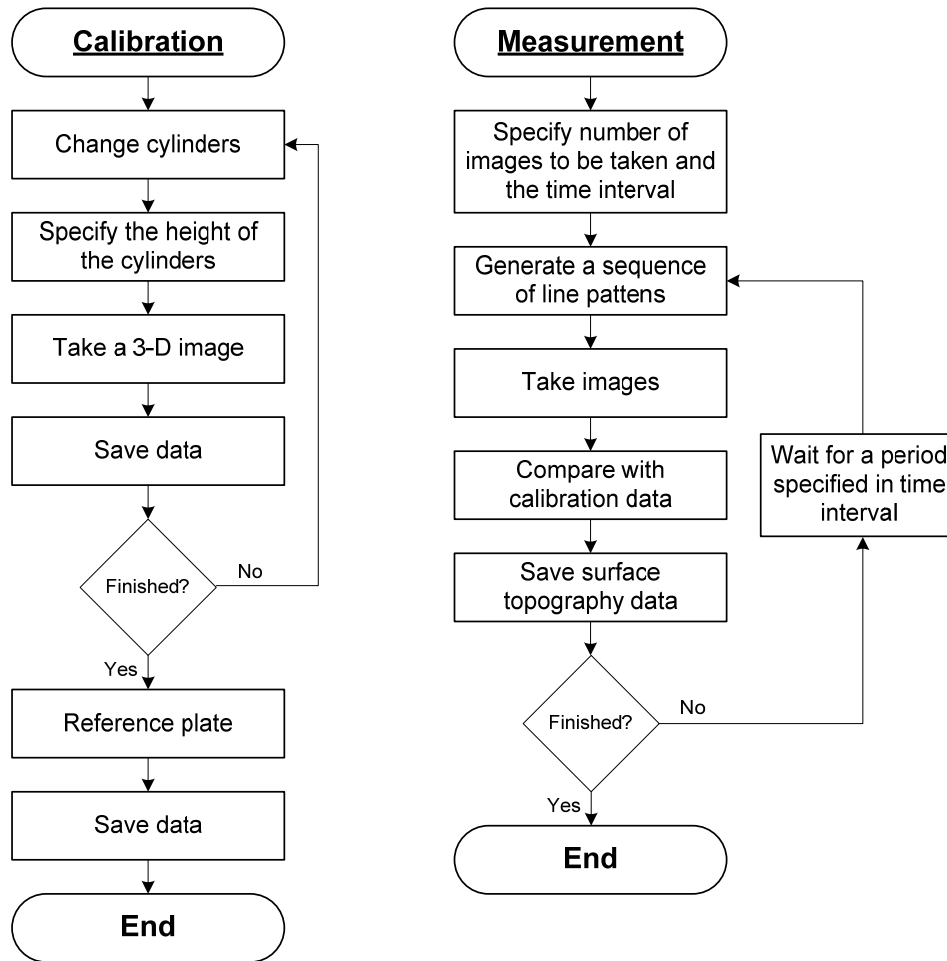


Figure 11: Program flow chart of the calibration of the image system and measurement of curl in a sample

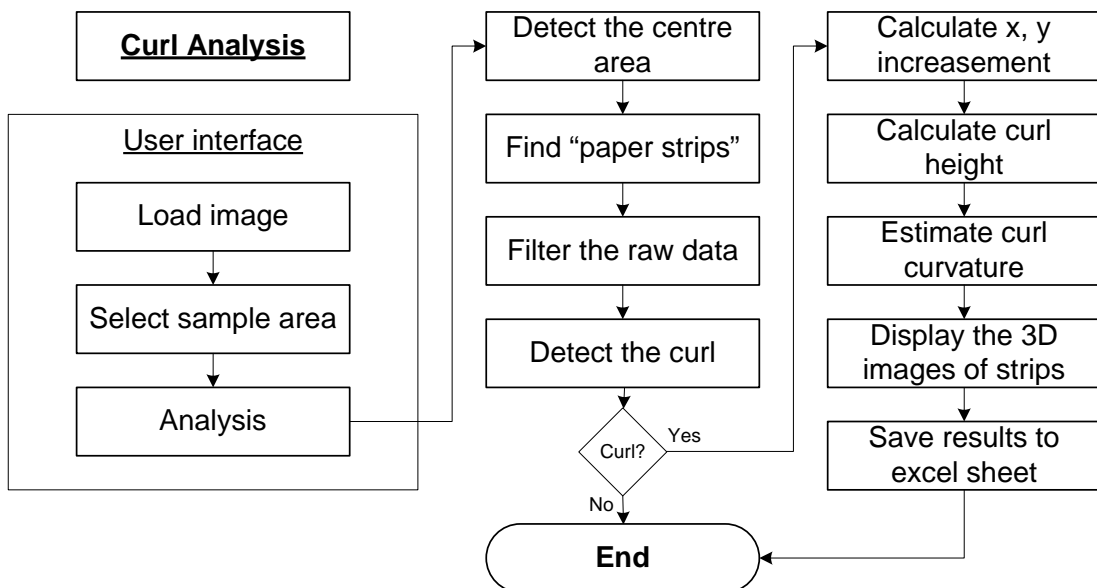


Figure 12: Program flow chart of the curl analysis software

4.1.3 Measurement procedures

The workflow of the analysis is as follows:

- The paper sample is conditioned in the standard air-conditioning room for 24 hours according to TAPPI standard T402 sp98.
- The paper sample is die-cut into star shape.
- The paper sample is placed in a climate chamber and subjected to high humidity for 10 minutes.
- The climate chamber is then opened. The paper sample is exposed to the air in the standard air-conditioning room. The dynamic curl of the paper sample can be measured successively in an interval of as short as 30 seconds.

The time 10 minutes for conditioning the paper sample at high humidity is good enough for paper grades with low basis weight about 50 g/m². If a higher grammage paper is to be measured, longer time of conditioning must be used. The reason is explained in Chapter 5.3.3.

4.2 Climate chamber for sample treatment

The climate chamber can treat the paper sample at different air conditions, i.e., different levels of relative humidities. The bottom part contains about 3 litre salt solution which gives a constant relative humidity to the air over it. Some of the salts which can supply constant humidity are listed in Table 1.

Table 1: Constant humidity solutions [47]

Compound	Temperature range (°C)	RH 25 °C	A	B
KOH·2H ₂ O	5 - 30	9	0.014	1924
MgCl ₂ ·6H ₂ O	5 - 45	33	29.26	34
Ca(NO ₃) ₂ ·4H ₂ O	10 - 30	51	1.89	981
NaCl	10 - 40	75	69.20	25
KCl	5 - 25	84	49.38	159
K ₂ SO ₄	10 - 50	97	86.75	34

The constant relative humidity (RH) produced by the salt solution at certain temperature can be calculated according to:

$$RH = A \exp\left(\frac{aB}{T} - \frac{b}{T}\right) \quad (3)$$

where A and B are constants for each salt solution as shown in Table 1, and T is the temperature in Kelvin.

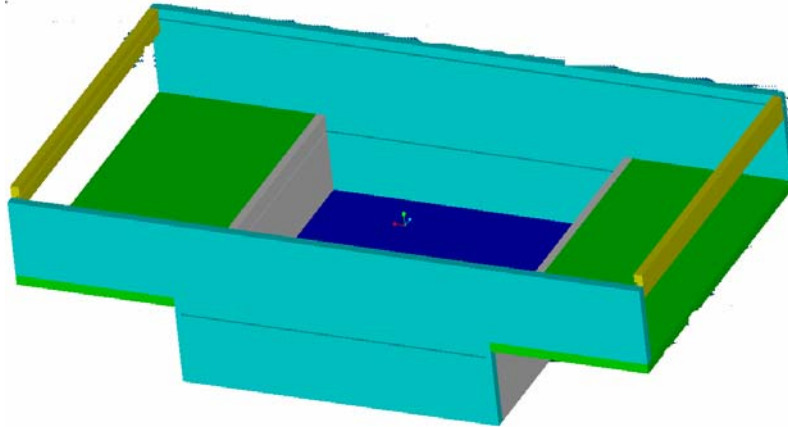


Figure 13: Schematic diagram of the climate chamber[48]

The upper part of the climate chamber is separated from the bottom part by a drawable stainless steel plate, above which an aluminium screen is placed. During the measurement of paper curl, the paper sample is put on the screen. Therefore, the paper sample can be exposed to the humidity determined by the salt solution in the bottom part when the steel plate is open.

On the top of the climate chamber, there is a removable glass cover. It offers a possibility to exchange the humid air with the surroundings in a constant standard conditioning room, while permit the light transmit required by the imaging system.

There are openings at the two sides of the chamber. They are designed for fast change of air humidity inside the chamber with the supply of external air sources with desired relative humidities.

4.3 Operation of the imaging system

The key components of the imaging system are the line projector and the CCD camera. The “coded light” procedure is employed in the measurement system. The line projector generates a sequence of line patterns (Figure 15) and cast them onto the surface of the object of interest. The lines are distorted according to the surface shape of the object. Immediately the distorted lines are captured by the camera and transmitted to the analysis software. The analysis

software interprets the line patterns by comparing them with pre-recorded calibration data and gives the three dimension information of the object.

4.3.1 Principle of coded light procedure

To illustrate the operation principle of the coded light procedure, we begin with considering a simple case where only one dark line is generated and cast by the projector onto the surface of the object in question. As can be seen from Figure 14, when a straight dark line (shown as red line in the figure) generated by the projector hits the surface of the object from an angle α with respect to the horizontal basis, it distorts into a curve following the shape of the surface of the object. The CCD camera located at a position with an inclined angle β captures the deformed dark line.

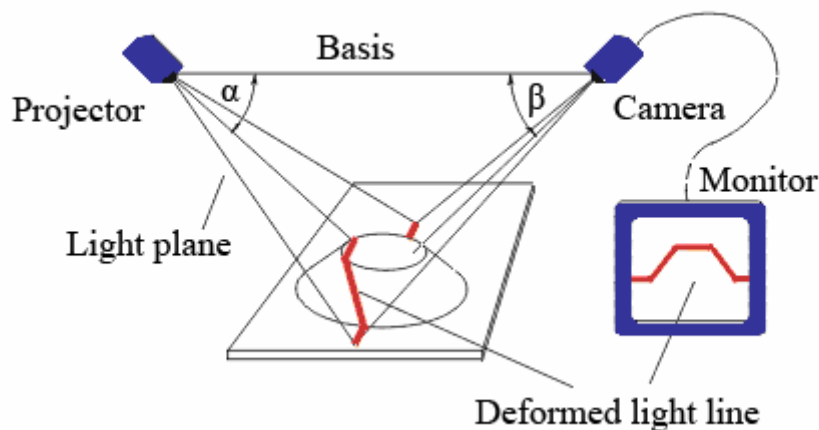


Figure 14: The coded light principle

If the position of the light source, the orientation of the light plane (α), and the position and orientation of the camera (β) are all known, a vision system can calculate the position of each of the points on the dark line in three dimensions.

For the measurement of the surface topology of an object, many dark lines with varying angle α of the incident light must be generated to cover the whole surface of the object. Consequently, each situation of a varied angle α , one image has to be taken by the camera. Obviously, it takes very long time to finish one measurement.

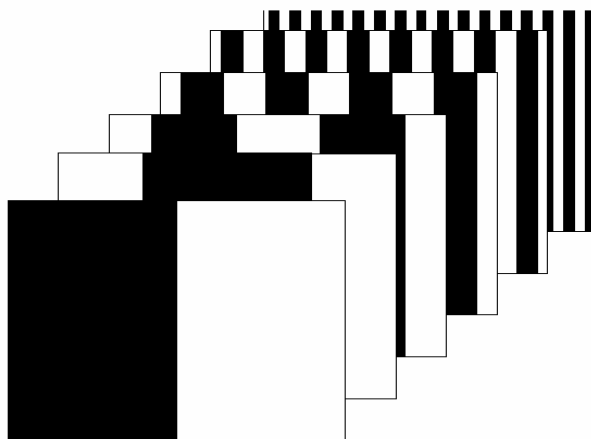


Figure 15: Line patterns generated by the line projector

To promote the measurement process, instead of generating one dark line at a time, a series of dark line patterns as shown in Figure 15 is generated. For each line pattern, one image is captured. The line patterns are a series of alternating black and white lines with varying line width for each pattern. The patterns are sequentially cast on the surface of the object.

One of the substantial advantages of the coded light procedure in comparison to other techniques is the speed. With this procedure, the three-dimensional measurement can be accomplished by inspecting the object surface.

4.3.2 Application of the coded light method for curl measurement

The curl detecting system consists of three main components, the line projector, the CCD camera and the climate chamber. The line projector generates coded line patterns. The CCD camera observes the line patterns distorted by the curled surface of the paper sample. The climate chamber has a wire supporting the paper sample. The high humidity generated by the salt solution beneath the wire can be introduced to the paper surface. The paper sample then absorbs the moisture from the damp air until it reaches equilibrium governed by the sorption isotherm of the paper.

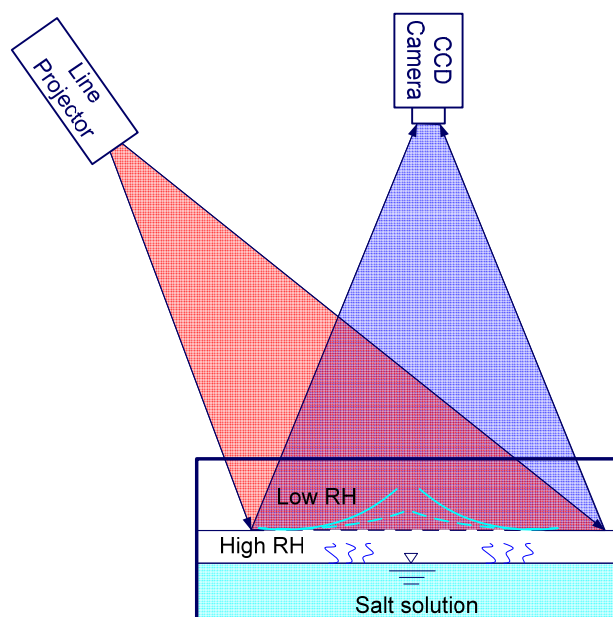


Figure 16: Setup of the curl detecting system

In the application of curl measurement, the line projector and CCD camera are arranged in this way: the line projector is aligned at an angle of 30° from the horizontal plane, while the CCD camera is placed perpendicularly over the paper sample. This arrangement offers very good measurement accuracy with low level of noise.

4.3.3 Calibration of the imaging system

Since it is not so easy to measure exactly the positions of the line projector and the camera as well as the inclination angles α and β , the surface topology calculation has been modified in our curl measurement application, so that the knowledge of those parameters is not necessary.

The system is calibrated before a curl measurement. If the system has not been moved, no re-calibration is required. The purpose of the system calibration is to build up a three dimensional map of the measurement space. After calibration, the surface topology of any object inside the measurement space can be obtained by comparing with the three dimensional map.

The system calibration involves a dozen of metal cylinder sets (four cylinders in a set) and a plate with equally distributed print circles on the surface. The cylinders support the climate chamber from its four corners.

Each of the twelve sets of metal cylinders used for calibration consists of four surface polished cylinders of precisely the same height. During the system calibration, the metal cylinders are changed gradually set by set from the lowest to the highest in height while the calibration plate inside the climate chamber where the paper sample is to be placed. A sequence of images is taken for each change of the calibration set. After the system calibration, a discrete three dimensional map is obtained and stored for later use, e.g., during curl measurement. Depends on the required precision of the system, the number of the calibration sets can be increased and the height difference between each consecutive two sets can be decreased.

4.4 Sample preparation

After trials with several types of sample geometries, we concluded that strips in CD, MD and diagonal direction from a paper sheet can best reveal the potential curl behaviour of a paper sample in the corresponding directions. If we cut the paper into real strips, we must mark each strip regarding its location on the paper sheet and to which direction they were cut. That makes the sample preparation a tedious work for the operator. Therefore we developed an H-shape cutting, which produces many “strips” on a single paper sheet without actual separation them from the sheet.

The H-shaped strips can be made by hand with a knife and a ruler. The edge sharpness and length of the strips made in this way, however, depend largely on the operator’s skill. As a matter of fact, the curling behaviour of a strip is influenced to a great extent by its edge sharpness. Therefore, a consistent uniform cutting offered by die-cutting machine is desired.

Being able to obtain as much information as possible from a single piece of paper sample can obviously promote the experimental speed and save material because the curl measurement is a destructive measurement. The arrangement of the strips on a paper sample can be optimized to have maximum number of strips on a given size of paper sample. The optimization work is accomplished with the star-shape cutting. The total number of strips that can be made on a piece of paper sample is limited by the size of the paper sample, which is restricted to 180 mm

× 180 mm, that is the limitation exposed by the CCD camera which has such a sensible size in our setup.

4.4.1 H-shape die-cutting

With one H-shape cut, we get two paper strips. Each of them has one free end. The other ends are still fixed in the paper sample. With such kind of configuration, the geometric information – the location and direction – of each strip is retained during even after the curl measurement.

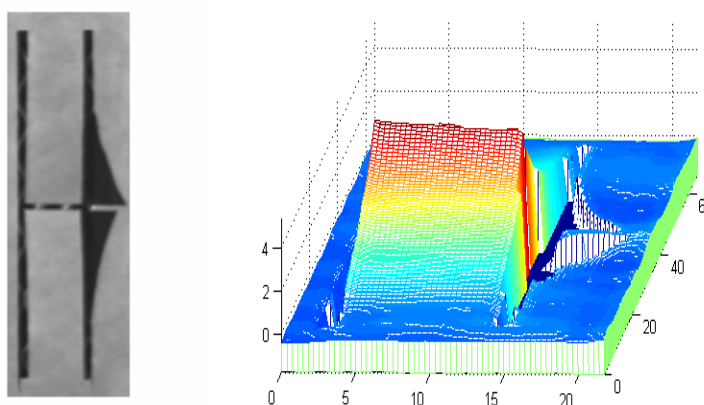


Figure 17: The 2-D (left) and 3-D (right) images of the curl formed on strips with a typical H-shape cut

The size of each strip is 30 mm in length and 10 mm in width. Since these strips are not really separate from the base paper sample, the curl behaviour in the strips is influenced by the reaction of the base paper sample. For example, if the free end of a strip curls up, the base paper must be able to balance the force introduced by the weight of the curled-up strip at the free end. Therefore, each fixed end of the strips must be restricted from any possible out-of-plane movement. This is achieved by placing a heavy metal plate at the fixed end.

4.4.2 Star-shape die-cutting

Paper samples are die-cut into star shapes with symmetric tips of size 30 mm in length and 10 mm in width (Figure 18). The die-cut can prevent the mechanical damage to the edges of the shape, which can, otherwise, affect the form of the curl in paper.

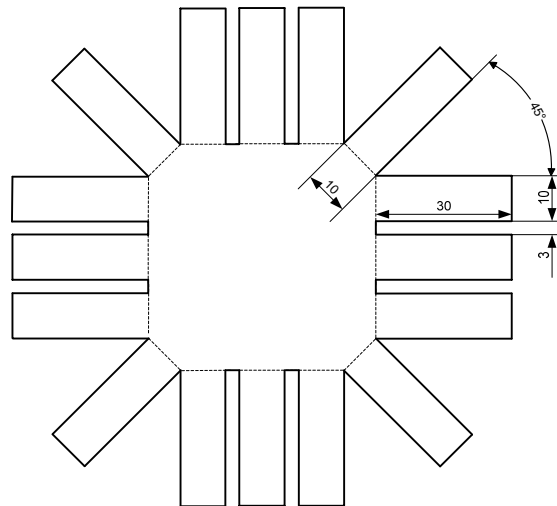


Figure 18: The star-shape die-cutting template

With such star shape cut, if there are curls in any directions (CD, MD or diagonal) can form independently. Consequently, they can be detected by the imaging system simultaneously. Therefore, curl in three dimensions can be measured with single run.

For the same reason as of the sample prepared with H-shape cutting, the centre of the star-shape paper sample is covered with a heavy metal plate to prevent any possible out-of-plane movement of the paper caused by the curling force introduced by the weight of curled-up strips at the free ends. The shape and size of the metal plate is shown as dotted line in Figure 18.

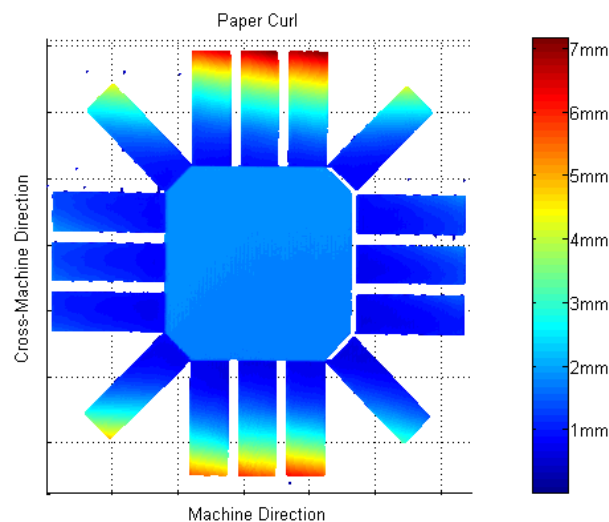


Figure 19: Typical curls in a paper sample die-cut in star shape

It is well known that the tendency of paper curl in CD direction is much higher than in MD direction, which is a result of that fibre orientation in a machine-made paper dominates in MD

direction. As shown in Figure 19, the strips in CD direction have severe curls, while those in MD direction show no detectable curl. From the colour gradient in the diagonal strips, we can observe curl in CD direction instead of diagonal direction.

4.5 Treatment of the paper sample

The curl in paper may appear when it is in an environment with varying humidities. The degree of the curl curvature depends on the history to which the paper has been subjected [8]. If the paper sample is subject to the cyclical humidity change starting from moisture desorption, it takes long time to reach stable state (the curvature change is more or less “reversible”) because it has to undergo several humidity cycles (see Figure 20). On the contrary, if the sample is treated with a humidity change starting from adsorption stage, it is quicker for the sample to reach stable state regarding its curvature behaviour (see Figure 21).

Therefore, in the curl measurement procedure, the humidity cycle starting from adsorption is adopted. The paper sample is first exposed to a high humidity around 90% RH, and then to a low humidity close to 52% RH (controlled by the room condition).

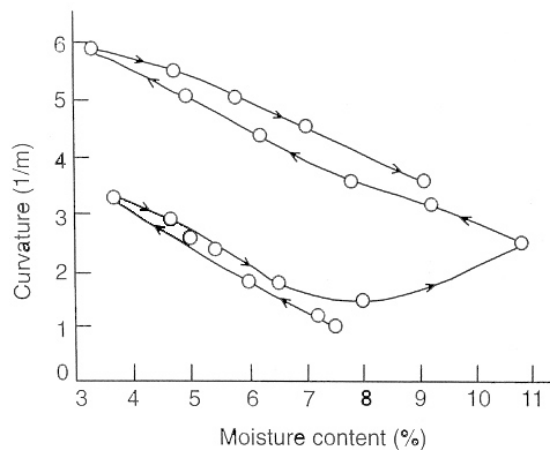


Figure 20: Bending curvature response to cyclical humidity changes when the process starts from the desorption stage

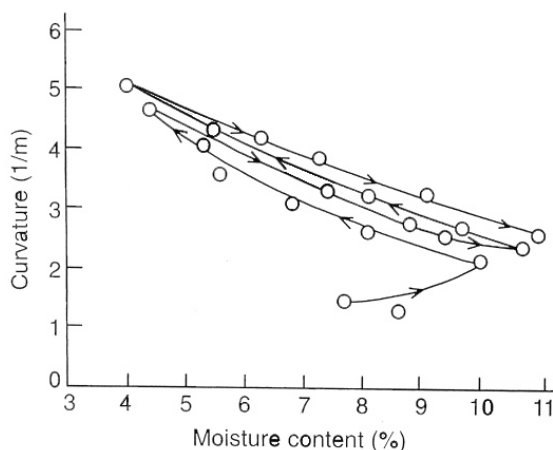


Figure 21: Bending curvature response to cyclical humidity changes when the process starts from the adsorption stage

During the curl measurement, the sample is treated by exposing to high relative humidity for ten minutes. For low grammage paper grades like newsprint, the process of adsorption and desorption of moisture is very fast. Our previous experiences indicate that it takes only few minutes for the moisture in paper to reach equilibrium with the environment. Therefore, ten minutes of processing time is long enough for this application. If the paper grammage is very high, for example, in the case of carton board or the sample has been coated so that it has low humidity absorption rate, the processing time should be increased accordingly.

4.6 Architecture of the curl measurement method

The architecture of the new curl measurement method based on image analysis techniques can be outlined as the block diagram shown in Figure 22. The image analysis techniques have been used intensively for obtaining the topography of paper surface with curl in the form of range image and for the analysis of the range image to interpret curvature of the sample.

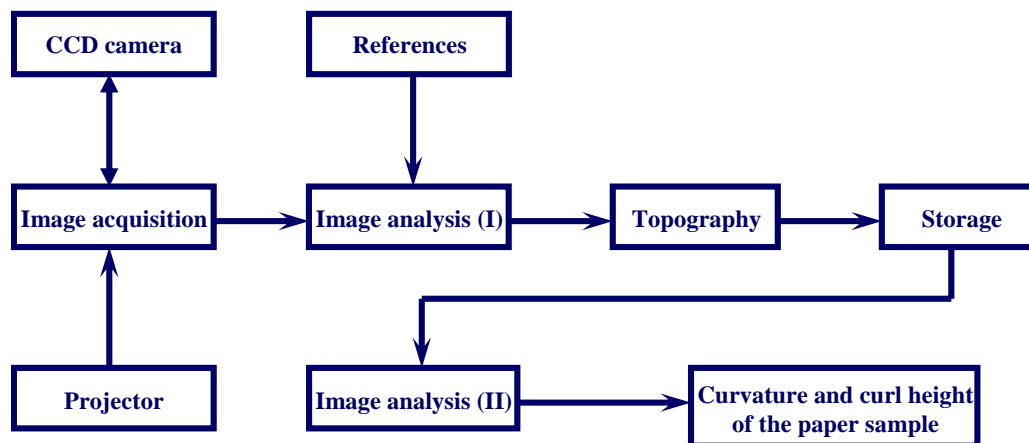


Figure 22: Curl measurement and analysis architecture

The curl measurement starts from the projecting of the coded line patterns triggered by the corresponding software. Simultaneously, the CCD camera shoots the image and transfers the image to the image analysis software (I). The image analysis software compares the received image with the calibration data (references) and gives the three-dimensional range image (surface topography of the curl). The range image is saved for further analysis.

From the save range image, another image analysis software developed in Matlab calculates the curvature and curl height of the paper sample and reports the results in excel forms. The detail of the calculation is discussed in next section.

4.7 Data pre-processing

The measurement data of the curl is a 3-dimensional image, which can be represented by three 2-dimensional matrices, namely, \mathbf{x} , \mathbf{y} and \mathbf{z} , they store the information of the locations of each points in Cartesian coordinate system. The height of each point is stored in the matrix \mathbf{z} as one element. Since noise is ubiquitous in every measurement system, the measurement data must be de-noised with a filter before further treatment. However, the useful information must be preserved as much as possible. Among many available methods, computational molecules can serve well for this application [49, 50].

The computational molecules are linear templates that added together to form a 3×3 averaging mask:

$$\begin{array}{|c|} \hline 1 \\ \hline \end{array} + \begin{array}{|c|c|c|} \hline 2 & 4 & 2 \\ \hline \end{array} + \begin{array}{|c|} \hline 2 \\ \hline 4 \\ \hline 2 \\ \hline \end{array} + \begin{array}{|c|} \hline 1 \\ \hline 2 \\ \hline 1 \\ \hline \end{array} = \begin{array}{|c|c|c|} \hline 1 & 2 & 1 \\ \hline 2 & 12 & 2 \\ \hline 1 & 2 & 1 \\ \hline \end{array}$$

According to the central limit theorem, the above 3×3 averaging mask must be normalized so its weights add to one. Then the result mask for filtering the range data becomes:

$\frac{1}{24}$	$\frac{1}{12}$	$\frac{1}{24}$
$\frac{1}{12}$	$\frac{1}{2}$	$\frac{1}{12}$
$\frac{1}{24}$	$\frac{1}{12}$	$\frac{1}{24}$

To avoid smoothing across discontinuities, the molecules crossing these discontinuities are not used and the remaining ones are once again normalized so the total sum of the weights is equal to one.

4.8 Identification of the height and the curvature of the curl

The magnitude of curl in paper can be characterized by the height of the curled paper edge (curl height) or the reciprocal of the radius of the curl (curvature). In this section the mathematical representation of these measures are scrutinised.

4.8.1 Curl height

The curl height is determined from the filtered range data. For each tip on a star shape paper sample, it is defined as the relative height of the tip in comparison with the base at the centre of the sample (Figure 23). It is designated as 'h' in the figure.

In Figure 23, the separated dots represent the measured height relative to the reference plate used during the calibration of the imaging system. The fitted curve is determined according to the curvature calculation defined by Eq. (4)–(7).

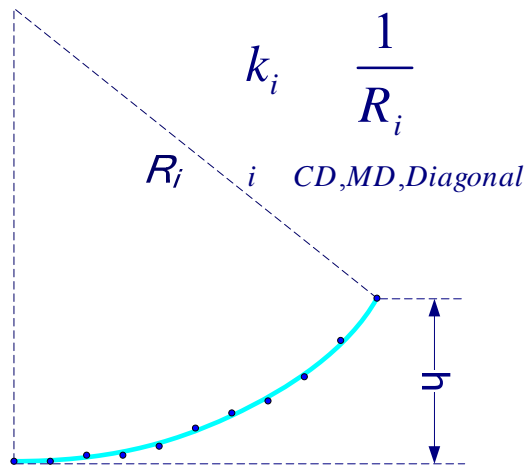


Figure 23: Height and curvature of a curl.

In determination of the curl height, the lowest point is well defined due to the fact that the base at the centre of the star shape sample is restricted from any out-of-plane movement by a metal plate covering over it.

4.8.2 Curvature of curl

The curvature of a curl can be determined directly from the definition of curvature, which is the reciprocal of the radius that the curved surface is lying on. It can also be derived from the geometrical shape of the curl. The later method makes use of only two parameters – the height of the curl and the projected length of the strip.

4.8.2.1 Direct evaluation method

As been discussed previously, paper can curl in three directions, namely, machine direction (MD), cross machine direction (CD) and diagonal. In each direction, the curl curvature can be expressed separately as:

$$K_i = \frac{1}{R_i} \quad (4)$$

where K_i – the curvature
 R_i – the radius of the curvature

According to Eq. (4), the curvature of the curl is the reciprocal of the radius of the circle which represents the curl. The radius of the circle can be identified as such,

Suppose there are n two-dimensional points (\mathbf{x}, \mathbf{y}) which are measured data with noise. Those points obey the equation of a circle,

$$(\mathbf{x} - x_0)^2 + (\mathbf{y} - y_0)^2 = r^2 \tag{5}$$

where, \mathbf{x}, \mathbf{y} – column vectors

(x_0, y_0) – the centre of the circle

r – the radius of the circle

Eq. (5) can be expanded and reorganized as:

$$\mathbf{x} \times 2x_0 + \mathbf{y} \times 2y_0 + (r^2 - x_0^2 - y_0^2) = \mathbf{x}^2 + \mathbf{y}^2 \tag{6}$$

Substitute $a = 2x_0, b = 2y_0, c = r^2 - x_0^2 - y_0^2$ into Eq. (6), and rearrange the equation into matrix form,

$$\begin{bmatrix} \mathbf{x} & \mathbf{y} & 1 \end{bmatrix} \begin{bmatrix} a \\ b \\ c \end{bmatrix} = \begin{bmatrix} \mathbf{x}^2 \\ \mathbf{y}^2 \\ 0 \end{bmatrix} \tag{7}$$

Eq. (7) is a system of linear equations; it can be easily solved by Gaussian elimination in Matlab. Because the number of the measurement points is much bigger than the number of parameters (three in this case, namely, $a, b,$ and c) to be identified the system of equations are strongly overdetermined. The results obtained are in the least squares sense to the system of equations.

Example

Let us consider an artificial case to see how well the estimation is by the direct evaluation method. Suppose we have a set of *measurement data* covered with random noise (isolated circles in Figure 24), apply the direct evaluation method to the data set we get the fitted circle (the green dotted line). The *measurement data* are in fact artificially generated by superimposing a random noise to a signal representing a half circle with known radius and the position of its centre (the solid red line).

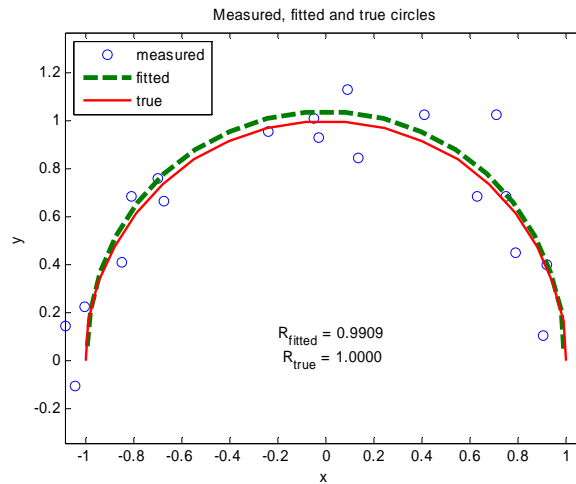


Figure 24: Circle fitting with direct evaluation method

It can be seen that the direct evaluation method gives rather good estimation of the circle radius, even though there are noises to both of the axes. The goodness of the circle fitting depends, of course, on the magnitude of the noise-to-signal ratio. If the noise-to-signal ratio is less than 5 %, the estimation error is also less than 5 %.

4.8.2.2 Indirect evaluation method

There is another method available to calculate the curl curvature which is given by Uesaka [8]. The calculation is based on the basic geometry of the curl assuming that the curl shape lies perfectly on a circle.

$$K_i = \frac{2Dy}{Dx^2 + Dy^2} \quad (8)$$

where K_i – the same as in Eq. (4)
 Dx – horizontal distance
 Dy – vertical distance

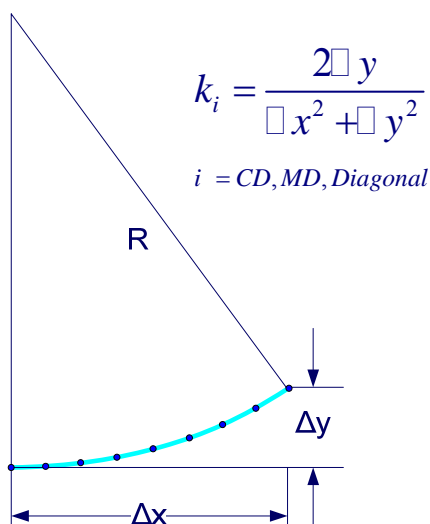


Figure 25: Curvature calculation – second method.

The advantage of this calculation method is that it guarantees the stability of the calculation. The drawback is that it can not distinguish whether there is a real curl or just a tilt flat sample. Therefore, the direct evaluation method is implemented in the final version of curl analysis software.

4.9 Dynamic curl

Curl in paper is usually measured at the state when the curl height or curvature reaches the maximum value. In some cases, the reaction time of curl may also be of interest to the customer of paper. For example, if the curl reaction time is much longer than the characteristic operation time of the process, it may not cause any problem to the process. Traditionally, it is not easy to measure curl behaviour dynamically. With the new measurement, however, this task becomes very easy and is done automatically.

During the curl measurement, the user is asked to specify the number of measurements and time interval between every two measurements required. The measurement is then run automatically. The analysis software makes use of the information and saves the time-dependent results of curl behaviour in paper into excel sheets.

5 Experimental work

The anisotropy and two-sidedness of paper physical properties such as hygroexpansivity and fibre orientation are regarded as the fundamental factors influencing the curl tendency of paper sheets. Other factors like basis weight may also have influence on the curl property of paper. To investigate the influences of these factors a serial of experiments were executed. A large amount of handsheets were made on RK (Rapid-Köthen sheet formers made by PTI) and M/K (M/K sheet formers made by M/K Systems Inc.) formers.

5.1 Laboratory sheets

Isotropic sheets (fibres are aligned randomly to all directions in the sheet plane) were made on RK former, while fibre highly oriented sheets were made on M/K sheet former. In addition, duplex sheets were made by pressing together two wet sheets, one made on RK former the other made on MK former, and then dried to have a single sheet with two plies.

In fact, the MK former is a simulator which can simulate the sheet forming process on a Fourdriner machine. The headbox discharges the evenly mixed stock onto a stationary wire under it at a small angle from one side of the wire. An overflow of the excess stock from the other side of the wire guarantees the stock is distributed evenly on the wire.

As been discussed previously in Chapter 3.1.2.1, the relative velocity difference between the stock flow and the wire makes the fibres aligned to the direction of the stock flow.

To investigate the influence of basis weight on the curl property of paper, laboratory sheets with varying grammages were made on the MK and RK formers.

5.1.1 Fibre properties

The laboratory sheets were made from various types of pulps, i.e., TMP (thermomechanical pulp), DIP (de-inked pulp), PGW (pressure groundwood pulp) and bleached sulfite pulp, which are commonly used in newsprint paper mills. The physical properties of these pulps were measured on FibreLab.

Table 2: Physical properties of the pulps used

Parameters	Units	TMP	PGW	DIP	Sulfite
Mean arithmetical fibre length	mm	0.70	0.40	0.52	0.94
Mean length weighted fibre length	mm	1.52	0.83	0.95	2.08
Mean mass weighted fibre length	mm	2.25	1.45	1.46	2.79
Fibre width	µm	28.85	22.90	21.95	27.5
Fibre wall thickness	µm	8.20	6.50	6.10	7.6
Fibre curl	%	14.20	20.80	19.83	19.6

Table 3: Grades of lab sheets made for curl analysis

		RK sheets	M/K sheets	Duplex
Grammage (g/m ²)	40	x	x	x
	60	x	x	x
	80	x	x	
	100	x	x	
	120	x		
Filler content (%)	0	x	x	x
	10	x		
	20	x		
	30	x		
Pulp type	DIP	x	x	x
	TMP	x		
	PGW	x		
	Sulfite	x		

5.2 Industrial paper samples

Newsprint papers were requested from paper mills. And they were sampled and delivery according to the following procedures:

1. Three strips were taken from the reel of the paper machine along CD direction. The dimension of each strip is 30 cm (in MD) × machine width.
2. The samples were marked as tending/drive side and top/bottom side.
3. To avoid the mechanical curl introduced by rolling up the samples, the paper samples were folded into 25 – 30 cm in width along CD direction.
4. To preserve the moisture in the paper, the paper samples were delivered in sealed plastic bags.

In addition, some special papers with known curl tendency by their manufacture, i.e., photo base papers were also requested and tested on the curl measurement system developed in this project to verify the workability of the system.

5.3 Measurement methods

As been discussed previously, hygroexpansion of paper and fibre orientation in the paper have great influence to the curl tendency of the paper. Therefore, both of them should be measured in order to investigate the influence of them to the curl of paper.

5.3.1 Hygroexpansion

Paper is a hygroexpansive material. It expands or contracts under different relative humidities in the surrounding air. That is the main reason for the curl in paper.

The hygroexpansivity of paper is measured according to DIN standard [51] in a device called *Paper Humidity Expansion Meter* produced by Prüfbau. For fibre-oriented paper, viz., M/K sheets, duplex sheets and machine-made paper, both MD and CD hygroexpansivities are measured.

5.3.2 Fibre orientation

It is nearly impossible to microscopically define an exact fibre orientation for a paper sheet (for example, papermaking fibres are usually curled or kinked, their orientation can be defined

in several ways). As a result, several methods have been developed for measuring apparent fibre orientation or main fibre orientation [52].

The apparent fibre orientation can be measured directly from the orientation of stained fibres in the paper sheet by means of image analysis technology. It can also be deduced by several indirect methods. One of which is TSO (Tensile Stiffness Orientation) test. As a matter of fact, TSO is basically an ultrasonic elasticity measurement [53, 54], but it does give a very good indication of fibre orientation in a sheet. In our case, the fibre orientation in the sheets was determined on Lorentzen & Wettre TSO Tester.

5.3.3 Effect of reaction time on curl

As the basis weight increases, the rigidity of paper increases accordingly. As a result, the magnitude of the maximum out-of-plane deformation (curl) is confined. In addition, it takes longer time for the moisture in the paper to reach equilibrium with the environment which relative humidity is changed. Consequently the time required to reach the maximum curl in paper is prolonged.

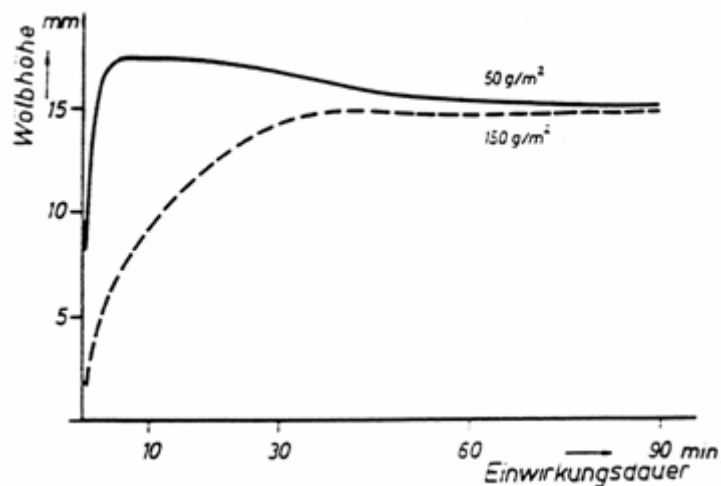


Figure 26: The influence of basis weight on the curl response of paper at 95% RH

For low grammage paper grade, e.g., 50 g/m², it takes very short time (few minutes) for the curl in paper to reach its maximum state (Figure 26).

6 Results and discussions

A novel curl measurement method based on image analysis technique has been developed. The technical details of this method are discussed in Chapter 4. In this chapter, the measurement and analysis results of curl in paper obtained by this method are presented.

6.1 Verification of the new measurement method

Immediately after the development of the new curl measurement method based on the image analysis technology, it was verified by measuring certain photo base papers which curl tendency are known to the manufacturer. The curl tendency of those paper grades are classified by the manufacturer as high curl, medium curl and low curl. Our measurement results follow exactly the same trend.

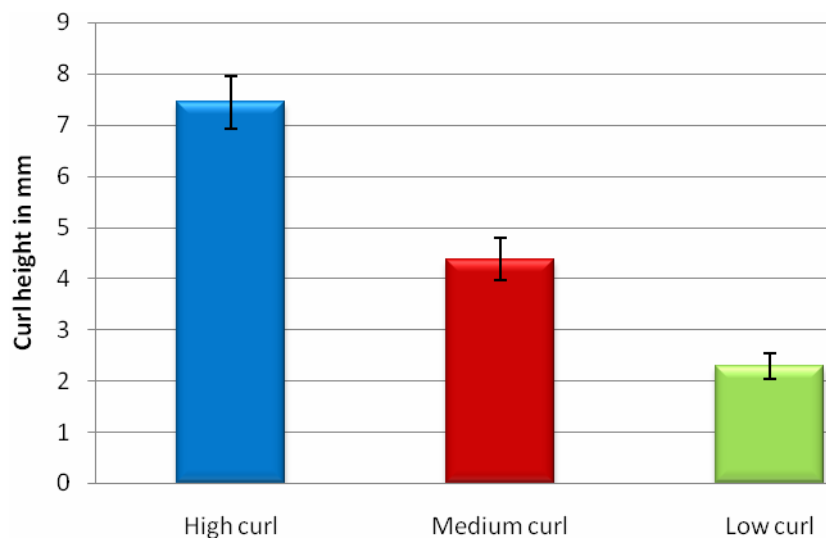


Figure 27: Curl of photobase papers

Since the photo base papers were obtained from indirect source, neither the raw material information nor the papermachine data are available. It is not possible to know the reason why those papers behave differently to curl. Anyhow, it is not of great concern to us because our aim is to verify the workability of the curl measurement system. The verification measurement results show that our system works very well as expected.

6.2 Relationship between curvature and curl height

As been discussed previously, the curl measurement and analysis system gives the results in terms of both curvature and curl height. They are, however, linearly correlated with each other (Figure 28).

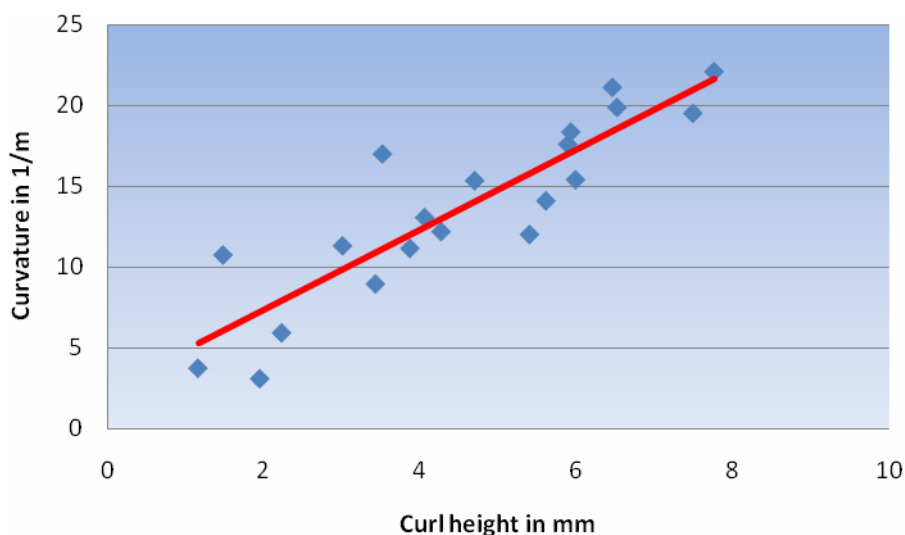


Figure 28: Curvature vs. curl height

It is found that the curl height and the curvature are correlated to each other provided that there is real curl in the area where examination was executed. If the shape is severely deviated from an arch shape, the standard deviation of the curvature estimation will be very high. This gives an indication whether the curl estimation of that area is reliable or not.

Consequently, the measurement and analysis results of curl have been presented in this report in the term of curl height exclusively.

6.3 Effect of fibre orientation on the curl in paper

To obtain fibre oriented sheets, M/K sheet former was used. To get a paper structure with biggest difference in fibre orientation in each “layer”, the duplex sheets were made by wet pressing RK sheets on the top of M/K sheets.

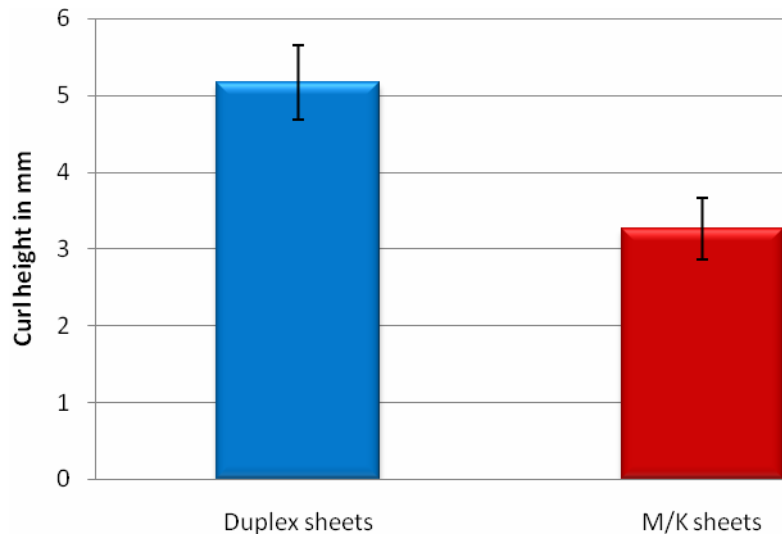


Figure 29: Effect of duplex sheets

Inhomogeneous fibre orientation is regarded as the most significant factor that influences the curl tendency of the paper. Paper sheets made on M/K former have very strong fibre orientation in MD direction. As a result, such sheets display a strong tendency to curl when they are subject to a circle of environmental humidity change. By contrast, there is no detectable curl in RK sheets, therefore, it is not show in Figure 29.

In comparison, the duplex sheet made by wet pressing one RK sheet over one M/K sheet has even stronger tendency to curl in the same condition. This is because the fibre orientation through the thickness of an M/K sheet is more uniform than that of a duplex sheet.

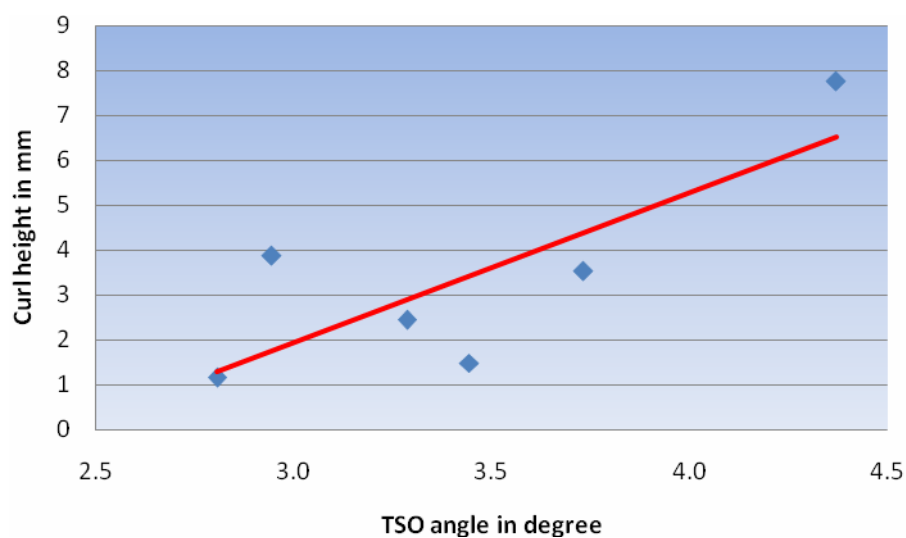


Figure 30: Influence of fibre orientation on curl

The quantitative relationship between fibre orientation and curl in paper is shown in Figure 30, where fibre orientation is measured as TSO angle in degree. As we can see, there is strong correlation between fibre orientation and the height of curl.

6.4 Effect of hygroexpansion on the curl in paper

Paper is a hygroscopic material, when it is exposed to an environment which has humidity different than that it has rested, it absorbs water vapour and expands or desorps and shrinks depending on the humidity difference between the two environments.

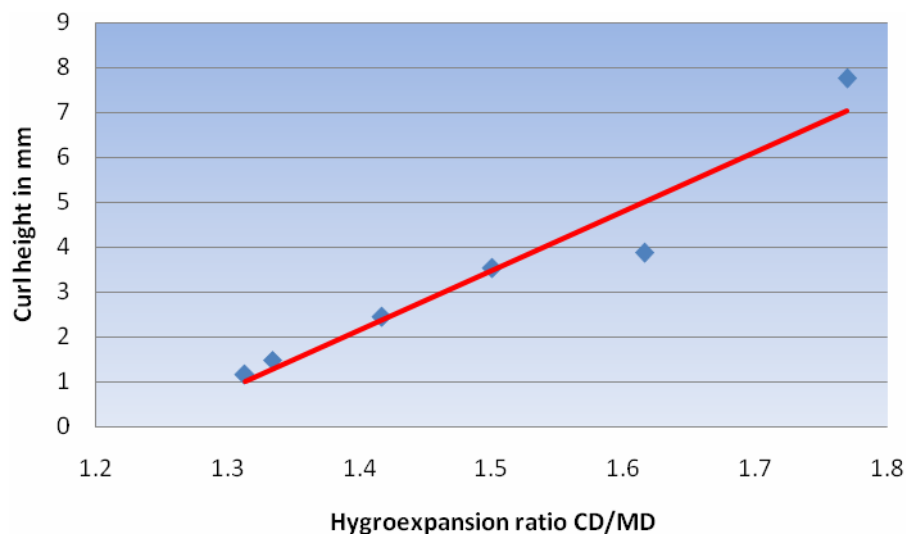


Figure 31: Effect of hygroexpansion on curl

It is well known that hygroexpansion has great influence on curl tendency of paper. Our experiment results strongly confirm this argument. In Figure 31, hygro-expansion was expressed in terms of a ratio of CD over MD. Theoretically, if the hygro-expansion is isotropic (equal in every direction) in paper, no curl should occur due to environmental humidity change. As the magnitude of anisotropy of hygroexpansion in paper increases, the curl tendency increases accordingly. This trend is strengthened by the hygroexpansion difference in thickness direction introduced by the duplex sheet.

6.5 Influence of basis weight on the curl in paper

As the paper basis weight increases, the thickness of paper increases correspondingly assuming that the density of the paper keeps constant. According to Eq. (9), the bending stiffness of paper increases when the paper thickness increases. Therefore, the out-of-plane deformation (curl) in paper is circumscribed within narrow bounds. As a result, low grammage paper has bigger magnitude of curl than high grammage paper does (Figure 32).

$$S_b = \frac{1}{12}Ed^3 \quad (9)$$

Where S_b – the bending stiffness of paper
 E – the elastic modulus of paper
 d – the thickness of paper

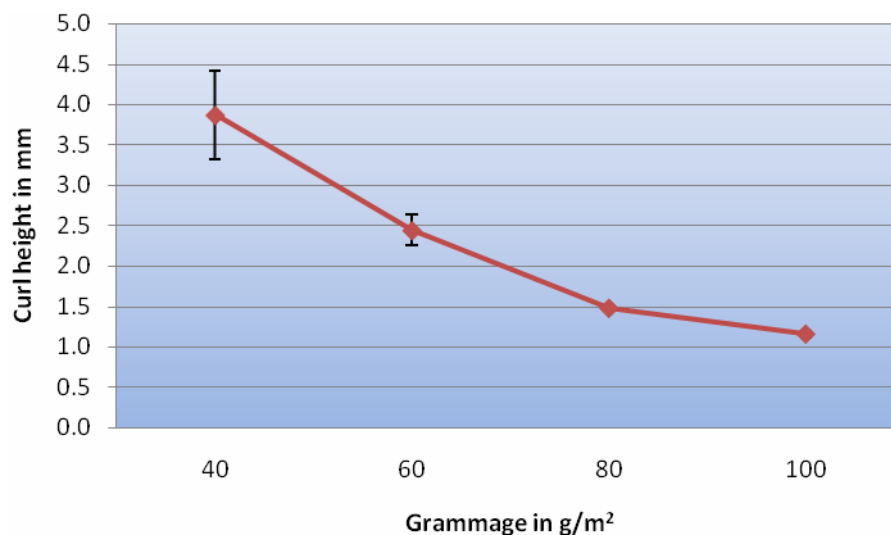


Figure 32: Influence of grammage (basis weight) on curl

In addition, it takes longer time for the curl to reach its maximum value (Figure 26) in high grammage paper. The curl measurement time must be extended accordingly.

6.6 Effect of cyclical humidity change on the curl in paper

In the humidity range between 50 % – 80 %, there is no significant change to the curl in paper under cyclical change of humidities. With a single cycle, curl has already approached its maximum value. Therefore, treatment of a paper sample with one cycle of humidity change is enough to get accurate and comparable value of the intrinsic curl in the paper.

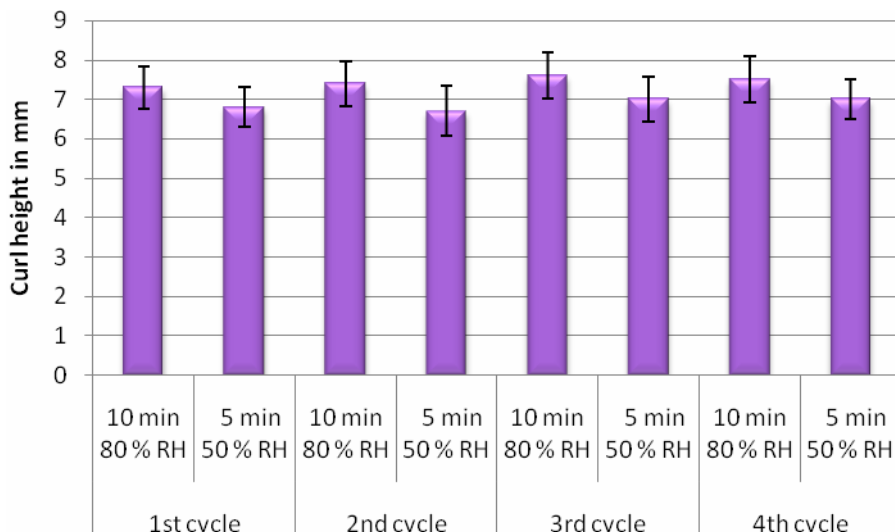


Figure 33: Curl und cyclical humidity change

6.7 Curl in newsprint

The measurement and analysis of curl in newsprint is a major task specified in the project proposal. It was expected to make correlation between the paper machine data as well as raw materials (the furnish) used and the curl tendency of the newsprint, because the curl was really a big problem to newsprint producers in the past. Nowadays, curl in paper has been quite well understood and the correction measures have been employed by most of the newsprint producers.

Anyhow, from one grade of newsprint, the CD profile of curl, TSI and TSO angle were measured. And the results are presented here.

The CD profile of curl in newsprint paper displays the same trend as many other paper properties' profiles, for example, tensile stiffness index (TSI) and tensile stiffness orientation (TSO) angle. The edges have stronger curl tendency than the center does. This is due to the fact that the cross flow at the edges on the forming wire is very significant. Therefore, the fibre orientation anisotropy along the thickness direction of the paper is the biggest at the edges of the paper web.

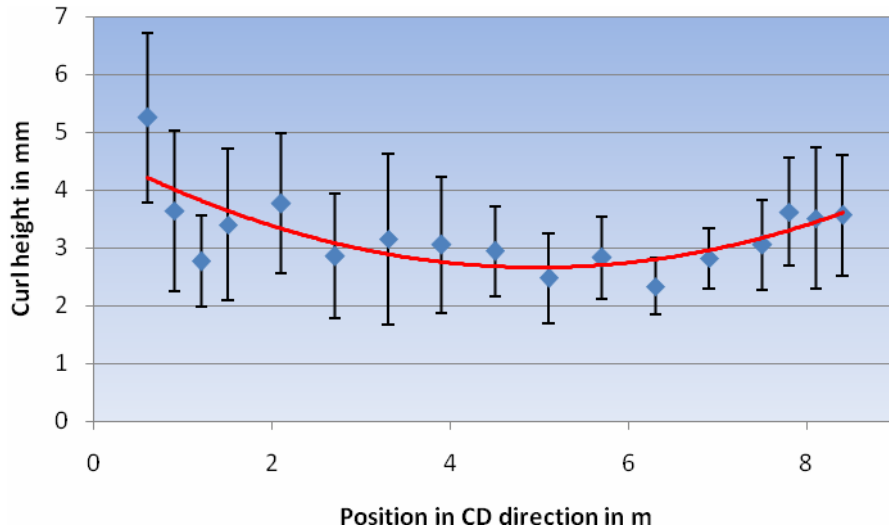


Figure 34: CD profile of curl in newsprint

The measurement of curl in newsprint displays rather big standard deviation for each location measured. This is due to the fact that the newsprint has big variation in local densities (poor formation). Consequently, it is subject to severe cockling problem. When we measure curl on a strip of dimension 10 mm × 30 mm, the curl measurement result is covered by the cockling effect to a large extent.

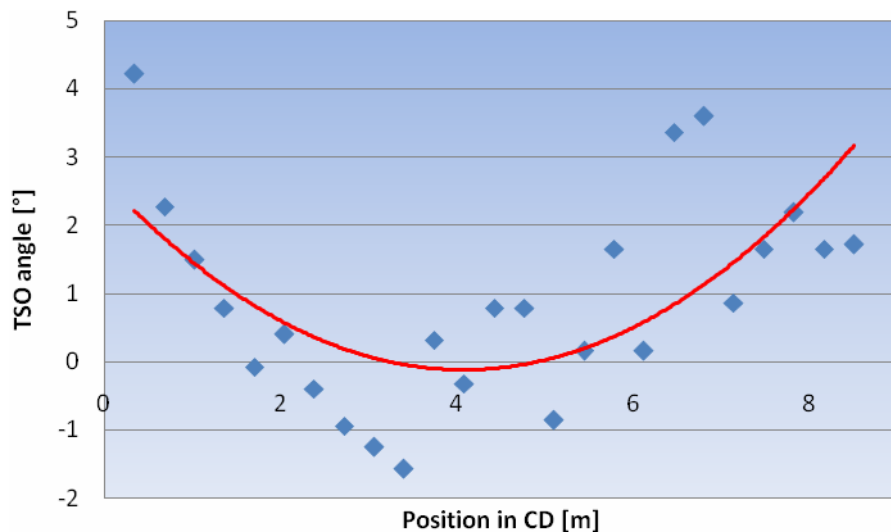


Figure 35: CD profile of TSO angle in newsprint

The measurement result of CD profile of TSO angle in newsprint shows big variations from place to place. This is because the paper sample was manually take from the machine reel. It

is possible that there are few degrees of mis-alignment of the sample in comparison with its real CD or MD direction when the TSO angle was measured.

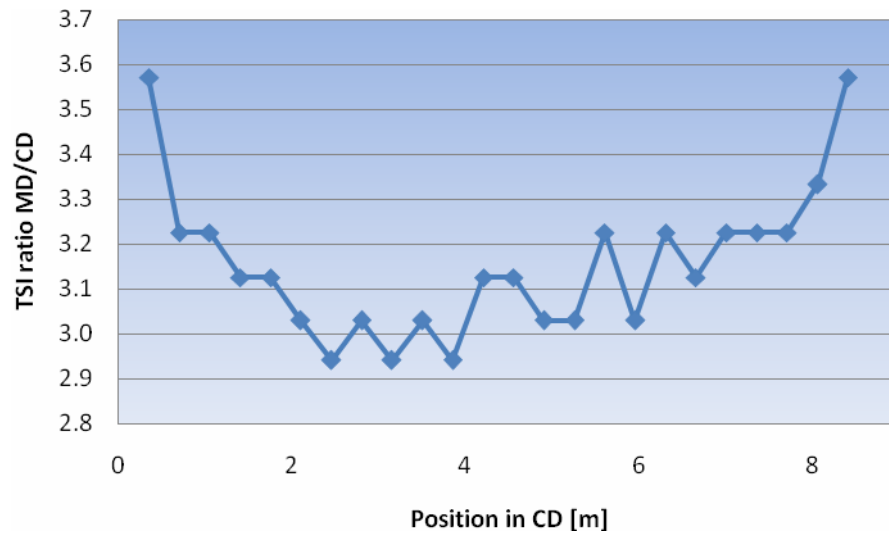


Figure 36: CD profile of TSI MD/CD ratio in newsprint

The CD profile of TSI MD/CD ratio in newsprint is rather smooth. This is because the TSI measurement is not sensitive to the exactness of the sample edges on CD and MD directions during the measurement of the TSI MD/CD ratio.

6.8 Measurement of dynamic curl

One great feature of the new curl measurement method is that it can measure dynamic curl behaviour of a paper sample. This is due to fast image sampling and processing frequency offered by the image measurement and analysis system.

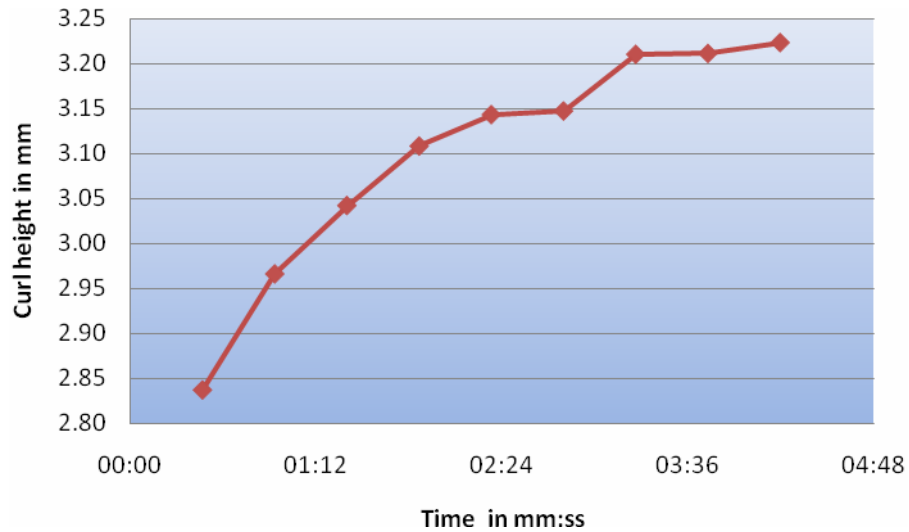


Figure 37: Dynamic curl in paper of basis weight 45 g/m²

Usually, curl in paper is measured at its maximum value in static state. From Figure 37, we see that it takes about 5 minutes for the curl in paper of basis weight 45 g/m² to reach its maximum. Therefore, the 5 minutes of processing time in our curl measurement procedure for paper grades of about 50 g/m² is justified.

7 Literature Cited

1. Rance, H.F., ed. *The Structure and Physical Properties of Paper*. Handbook of Paper Science: The Science and Technology of Papermaking, Paper Properties and Paper Usage. Vol. 2, 1982, Elsevier Scientific Publishing Company: New York.
2. Carlsson, L., C. Fellers, and M. Htun, *Curl and two-sidedness of paper*. Svensk Papperstidning, 1980. **85**(7): p. 194-197.
3. Bortolin, G., P.O. Gutman, and B. Nilsson, *On modelling of curl in multi-ply paperboard*. Journal of Process Control, 2006. **16**(4): p. 419-429.
4. Gallay, W., *Stability of dimensions and form of paper*. Tappi Journal, 1973. **56**(12): p. 90-95.
5. Nordström, A.L., P. Gudmundson, and L.A. Carlsson, *Influence of gravity on curl of horizontal paper sheets*. Tappi Journal, 2001. **84**(5).
6. Edwards, P.J., et al., *Paper curl prediction and control using neural networks*. Tappi Journal, 1999. **82**(7): p. 145-150.
7. Niskanen, K., ed. *Paper Physics*. Papermaking Science and Technology, ed. J. Gullichsen and H. Paulapuro. Vol. 16. 1998, Fapet Oy: Helsinki. 324.
8. Uesaka, T., *Dimensional stability and environmental effects on paper properties*, in *Handbook of Physical Testing of Paper*, R.E. Mark, et al., Editors. 2002, Marcel Dekker, Inc.: New York. p. 115-171.
9. Bristow, J.A. and P. Kolseth, eds. *Paper Structure and Properties*. International Fiber Science and Technology, ed. M. Lewin. Vol. 8. 1986, Marcel Dekker Inc.: New York. 390.
10. *TAPPI Technical Information Sheets (TIS 0108-01)*. 1989, TAPPI PRESS: Atlanta.
11. Olsen, J.A., *Analytic estimate of the fibre orientation distribution in a headbox flow*. Nordic Pulp and Paper Research Journal, 2002. **17**(3): p. 302-306.
12. George, H.O., *Methods of affecting the dimensional stability of paper*. Tappi Journal, 1958. **41**(1): p. 31-33.
13. Glynn, P. and W. Gallay, *Further studies on the mechanism of curl in paper*. Pulp and Paper Magazine of Canada, 1962. **63**(8): p. T418-424.

14. Salmén, L., et al., *The implications of fiber and sheet structure for the hygroexpansivity of paper*. Nordic Pulp and Paper Research Journal, 1987. **2**(4): p. 127-131.
15. Juppi, K. and J. Kaihovirta, *The effect of the dryer section on paper quality*. Pulp & Paper Canada, 2003. **104**(5): p. 58-61.
16. Niskanen, K., *Curl variations in paper and board*. Paperi ja Puu, 1996. **78**(5): p. 292-297.
17. Langevin, E.T. and W. Giguere, *On-line curl measurement and control*. Tappi Journal, 1994. **77**(8): p. 105-110.
18. Geenen, H., *Über die Behebung von Planlagestörungen bei ungestrichenen Papieren*. Wochenblatt für Papierfabrikation, 1986. **114**(3): p. 69-70.
19. Dahl, H., H. Holik, and E. Weissshuhn, *The influence of headbox flow conditions on paper properties and their constancy*. Tappi Journal, 1988. **71**(2): p. 93-98.
20. Nordström, A., P. Gudmundson, and L.A. Carlsson, *Influence of sheet dimensions on curl of paper*. Journal of Pulp and Paper Science, 1998. **24**(1): p. 18-25.
21. Brecht, W. and P. Räderer, *Das Rollen von Papieren in seiner Abhängigkeit von der Stoffbeschaffenheit*. Das Papier, 1965. **19**(6): p. 271-275.
22. Hendry, J.F., *Die Rollneigung von Papier*. Das Papier, 1962. **16**(4): p. 588-595.
23. Hendry, I.F., *Effect of machine variables on the curl of paper*. Paper Technology, 1963. **4**(4): p. T121-T128.
24. Astrom, M.E., R. Amiri, and D.G. Gray, *Chiral twisting curl of paper sheets - effect of fibre orientation*. Nordic Pulp and Paper Research Journal, 1994. **9**(1): p. 16-17, 25.
25. Bubik, A., *Betriebsergebnisse mit dem Escher Wyss Twinformer*. Wochenblatt für Papierfabrikation, 1986. **114**(21): p. 849-854.
26. Schoen, H., *Wechselwirkung zwischen Querprofilen am Beispiel einer Spezialpapiermaschine*. Wochenblatt für Papierfabrikation, 1995. **123**(5): p. 242-246.
27. Morris, V.A.P. and W.W. Sampson, *An investigation of heat curl in newsprint*. Tappi Journal, 1998. **81**(8): p. 191-194.
28. Brecht, W., P. Räderer, and W. Weitzel, *Über die Rollneigung von Papieren*. Das Papier, 1959. **13**(11/12): p. 237-244.
29. Shands, J.A. and J.M. Genco, *Cross-machine variation of paper curl on a twin-wire machine*. Tappi Journal, 1988. **71**(9): p. 165-169.
30. Pijselman, J. and J. Poustis, *Curl of multiply papers - an analytical study*. Svensk Papperstidning, 1982. **85**(18): p. R177-R184.

31. Uesaka, T., et al., *Curl in paper (2) Derivation of Approximate Curl Formulas and their Applicability*. Japan Tappi, 1987. **41**(4): p. 335-349.
32. Gray, D.G., *Chirality and curl of paper sheets*. Journal of Pulp and Paper Science, 1989. **15**(3): p. J105-J109.
33. Shands, J.A. and H.P. Frei, *A novel concept for cross direction basis weight control - a next generation headbox*, in *XXV Eucepa Conference*. 1993: Wien. p. 45-59.
34. Viitaharju, P., I. Kajanto, and K. Niskanen, *"Heavy" papers and curl measurement*. Paperi ja Puu, 1997. **79**(2): p. 115-120.
35. Nordström, A., L.A. Carlsson, and J.-E. Hägglund, *Measuring curl of thin papers*. Tappi Journal, 1997. **80**(1): p. 238-244.
36. Heinzmann, H., *Faserorientierungs-Querprofil*. Wochenblatt für Papierfabrikation, 1995. **123**(4): p. 121-126.
37. Chapman, J., D. Kole, and Å. Hellström, *Papermaking with new online fibre orientation measurement*. Paper Technology, 2000. **42**(4): p. 43-46.
38. Kohl, A. and W. Hartig, *Messung physikalischer Kenngrößen an laufenden Bahnen*. Das Papier, 1985. **39**(10A): p. V172-V177.
39. Koran, Z., J. Silvy, and R.E. Prud'homme, *Network structure and fiber orientation in paper*. Tappi Journal, 1986. **69**(5): p. 126-128.
40. Aidun, C.K. and A.E. Kovacs, *Hydrodynamics of the forming section: the origin of nonuniform fiber orientation*. Tappi Journal, 1995. **78**(11): p. 97-106.
41. Hutten, I.M., *Paper machine evaluation by fiber orientation profile analysis*. Tappi Journal, 1994. **77**(9): p. 187-192.
42. Aidun, C.K., *Hydrodynamics of steaks on the forming table*. Tappi Journal, 1997. **80**(8): p. 155-162.
43. Sze, D.H. and T.G. Waech, *Paper waviness and fiber alignment streaks in paper forming*, in *83rd Annual Meeting, Technical Section CPPA*. 1997: Montreal, Canada. p. A97-A103.
44. Söremark, C., G. Johansson, and A. Kiviranta, *Characterization and elimination of fiber orientation streaks*, in *Tappi Engineering Conference*. 1994. p. 97-103.
45. Meyer, H., *Hydrodynamics of the sheet-forming process*. Tappi, 1971. **54**(9): p. 1426-1450.
46. Parker, J.D., *The Sheet-Forming Process*. Special Technical Association Publication No. 9. 1972, Atlanta, GA.: Tappi. 104.

47. Lide, D.R., ed. *CRC Handbook of Chemistry and Physics, Internet Version 2005*, <http://www.hbcpnetbase.com>. 2005, CRC Press: Boca Raton, FL.
48. Jaeger, A., *Messung und Analyse der Rollneigung von Papier*, in *Fachgebiet Papierfabrikation und Mechanische Verfahrenstechnik*. 2005, Technische Universität Darmstadt: Darmstadt. p. 73.
49. Forsyth, D.A. and J. Ponce, *Computer Vision: A Modern Approach*. 2002: Prentice Hall. 693.
50. Kraus, K. and J. Schicho, *Algebraic Multigrid Based on Computational Molecules, 1: Scalar Elliptic Problems*. *Computing*, 2006. **77**(1): p. 57-75.
51. DIN 53 130, *Determination of dimensional stability (Bestimmung der Feuchtdehnung)*, in *DIN-Taschenbuch 213: Papier, Pappe und Faserstoff 2*. 2003, Beuth Verlag GmbH: Berlin. p. 46-47.
52. Titus, M., *Ultrasonic technology - measurements of paper orientation and elastic properties*. *Tappi Journal*, 1994. **77**(1): p. 127-130.
53. Loewen, S. and M. Foulger, *TSO and fibre orientation: an introduction*. *Pulp & Paper Canada*, 2002. **103**(5): p. 42-45.
54. Niskanen, K.J. and J.W. Sadowski, *Evaluation of some fibre orientation measurements*. *Journal of Pulp and Paper Science*, 1989. **15**(6): p. J220-J224.

8 Appendix A – Curl measurement results

Curl of photobase paper

	High curl	Medium curl	Low curl
Curl height in mm	7.44	4.38	2.29
Standard deviation	0.52	0.41	0.24

Effect of duplex sheet on curl

	Duplex sheets	M/K sheets
Curl height in mm	5.17	3.26
Standard deviation	0.48	0.40

TSI, TSO of lab sheets made of DIP

	M/K sheets				Duplex sheets	
Grammage [g/m ²]	40	60	80	100	47	54
TSI ratio MD/CD	1.74	1.69	1.68	1.60	1.32	1.29
Standard deviation	0.04	0.03	0.01	0.04	0.07	0.03
TSO angle [°]	2.94	3.29	3.44	2.81	4.37	3.73
Standard deviation	0.82	1.02	0.67	0.92	0.21	0.61

Hygroexpansion of lab sheets

	M/K sheets				Duplex sheets		RK sheets	
Grammage [g/m ²]	40	60	80	100	47	54	78	117
MD	0.13	0.12	0.12	0.16	0.13	0.10	0.11	0.11
CD	0.21	0.17	0.16	0.21	0.23	0.15	0.12	0.11
CD/MD	1.62	1.42	1.33	1.31	1.77	1.50	1.09	1.00

Curl in lab sheets

	M/K sheets				Duplex sheets	
Grammage [g/m²]	40	60	80	100	47	54
Curl height in mm	3.87	2.44	1.48	1.16	7.76	3.52
Standard deviation	0.55	0.19	0	0.04	0.63	0.08

CD profile of curl in Newsprint

CD position in m	0.6	0.9	1.2	1.5	2.1	2.7	3.3	3.9	4.5
Curl height in mm	5.25	3.64	2.76	3.4	3.77	2.85	3.15	3.05	2.94
Standard deviation	1.47	1.39	0.79	1.31	1.22	1.08	1.47	1.18	0.78
CD position in m	5.1	5.7	6.3	6.9	7.5	7.8	8.1	8.4	
Curl height in mm	2.47	2.83	2.33	2.82	3.05	3.62	3.51	3.56	
Standard deviation	0.78	0.71	0.49	0.52	0.77	0.93	1.22	1.05	

Curl under cyclical humidity change

	1st cycle		2nd cycle		3rd cycle		4th cycle	
	10 min 80 % RH	5 min 50 % RH						
Curl height (mm)	7.3	6.8	7.4	6.7	7.6	7	7.5	7
Standard deviation	0.54	0.5	0.57	0.63	0.58	0.58	0.58	0.5

CD profile of TSO and TSI in Newsprint

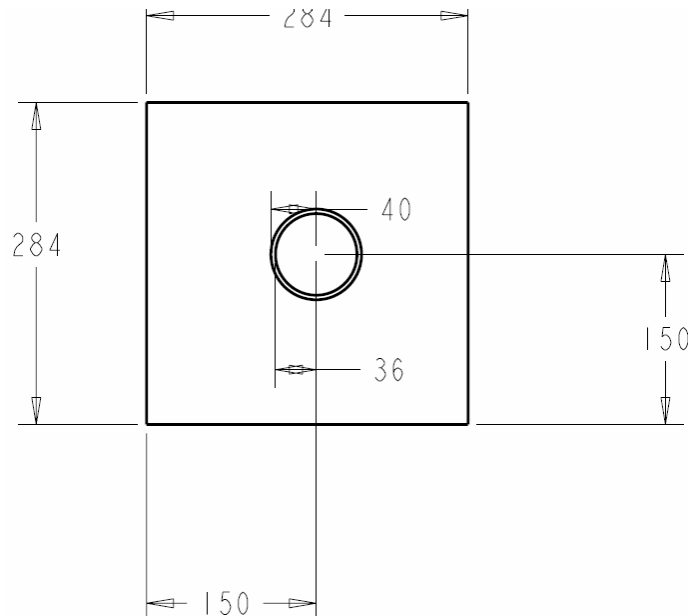
CD Position in m	0.35	0.7	1.05	1.4	1.75	2.1	2.45	2.8	3.15	3.5	3.85	4.2
TSO angle in degrees	4.22	2.27	1.49	0.79	-0.08	0.4	-0.4	-0.94	-1.25	-1.57	0.32	-0.32
TSI ratio MD/CD	3.57	3.23	3.23	3.13	3.13	3.03	2.94	3.03	2.94	3.03	2.94	3.13
CD Position in m	4.55	4.9	5.25	5.6	5.95	6.3	6.65	7	7.35	7.7	8.05	8.4
TSO angle in degrees	0.79	0.79	-0.86	0.16	1.65	0.16	3.36	3.6	0.86	1.65	2.19	1.65
TSI ratio MD/CD	3.13	3.03	3.03	3.23	3.03	3.23	3.13	3.23	3.23	3.23	3.33	3.57

Dynamic curl in newsprint

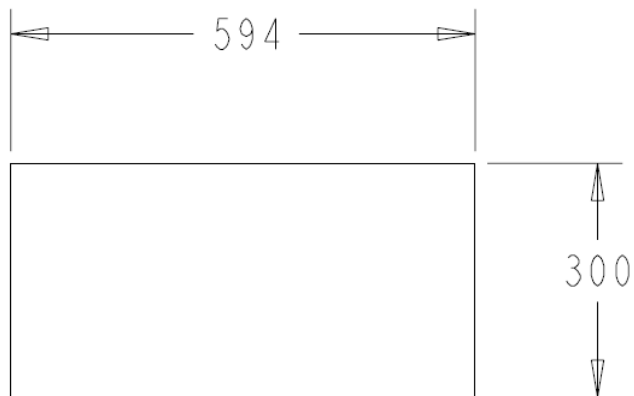
Time in mm:ss	00:28	00:56	01:24	01:52	02:20	02:48	03:16	03:44	04:12
Curl height in mm	2.837	2.966	3.042	3.108	3.143	3.147	3.21	3.211	3.223
Standard deviation	0.21	0.244	0.455	0.55	0.626	0.674	0.656	0.671	0.688

9 Appendix B – Drawings of the climate chamber

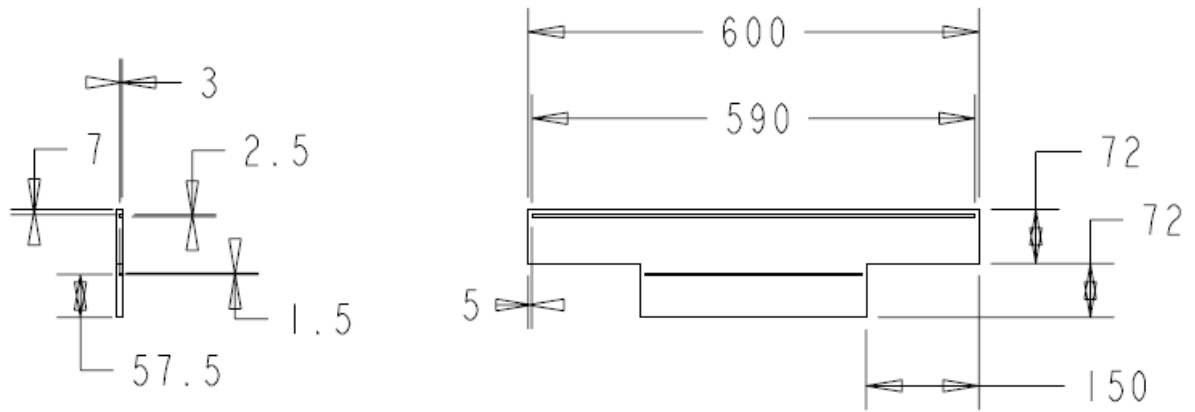
Bottom panel



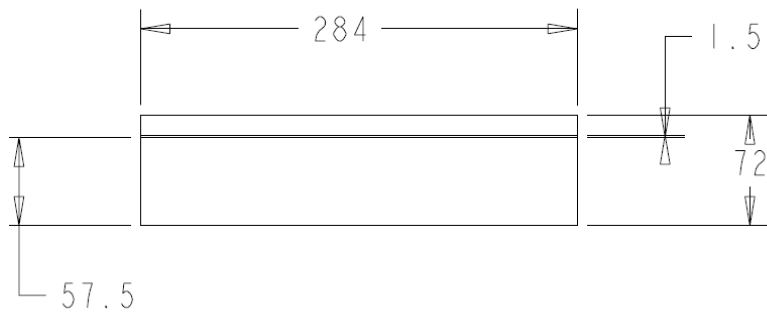
Glass plate



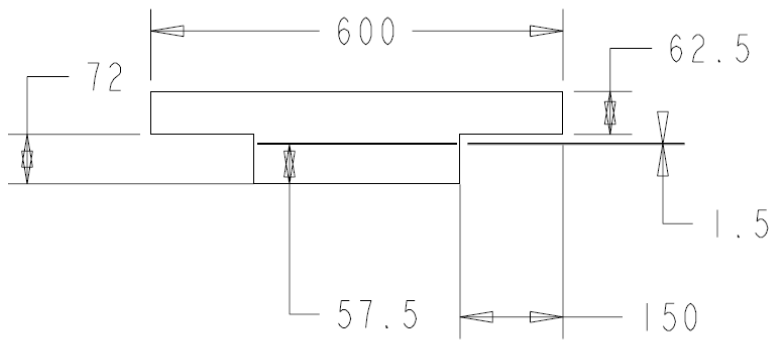
Rear panel



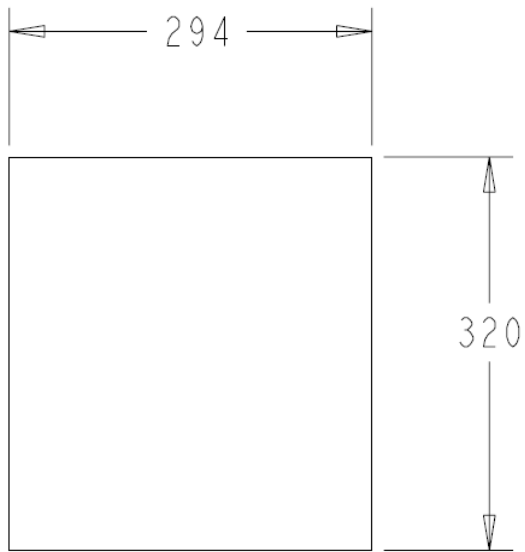
Left and right side panels



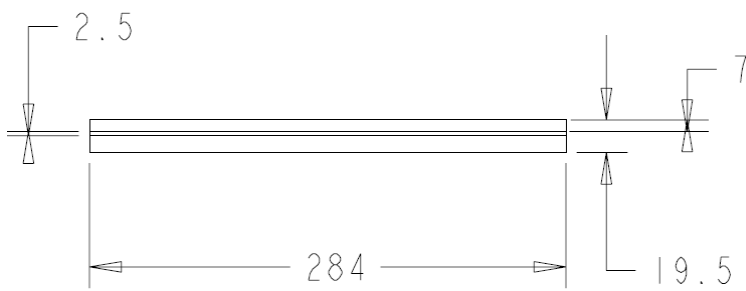
Front panel



Drawable metal plate

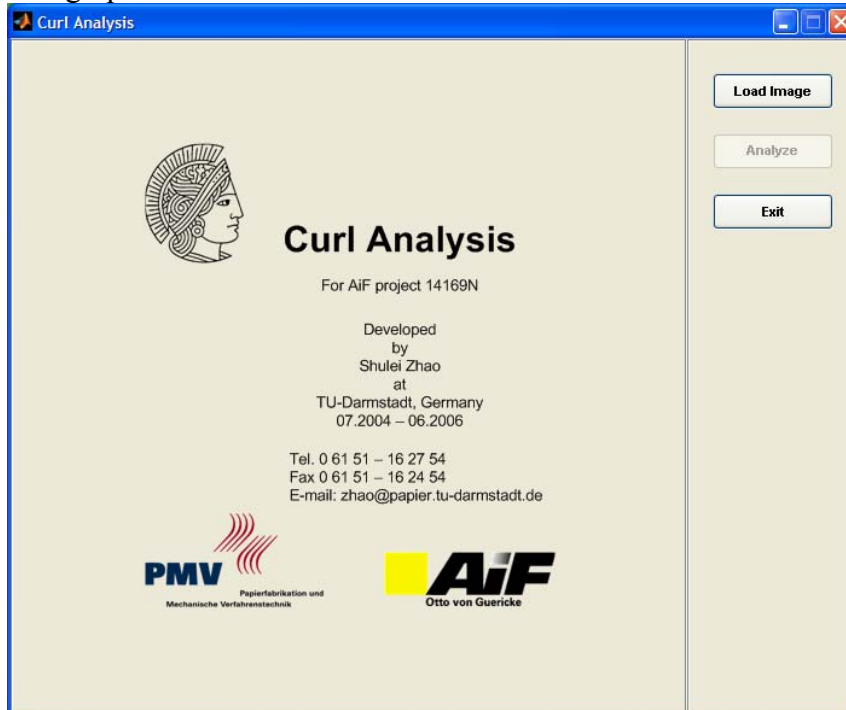


Left and right side bars

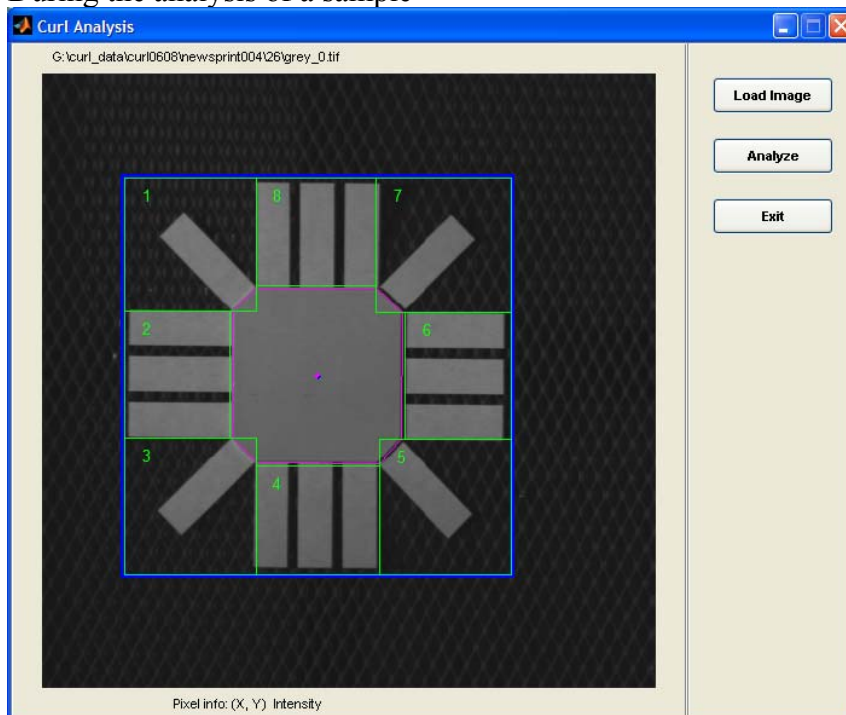


10 Appendix C – GUI of the Curl Analysis Program

The graphical user interface



During the analysis of a sample



11 Appendix D – Source Codes

11.1 Calibration program

```
# This program is to calibrate the imaging system.
```

```
#####
```

```
# Framebuffers
```

```
#####
```

```
# Framegrabber
```

```
# It is an Object to save Images
```

```
framebuf fb {  
    string  type,  
    string  config,  
    float   range[2],  
    short   live,  
    short   videoin,  
    short   sync  
};
```

```
fb.type     = "pc_eye1";
```

```
fb.config   = "cvm10.dat";
```

```
fb.range    = {0,255};
```

```
# Display of x coordinates
```

```
framebuf fbx {  
    string  type,  
    short   dispsize[2],  
    float   range[2]  
};
```

```
fbx.type     = "win";
```

```
fbx.dispsize = {512,512};
```

```
fbx.range    = {-400,400};
```

```
# Display of y coordinates
```

```
framebuf fby {  
    string  type,  
    short   dispsize[2],  
    float   range[2]  
};
```

```
fby.type     = "win";
```

```
fby.dispsize = {512,512};
```

```
fby.range    = {-400,400};
```

```
# Display of z coordinates
```

```
framebuf fbz {  
    string  type,  
    short   dispsize[2],  
    float   range[2]  
};
```

```
fbz.type     = "win";
```

```
fbz.dispsize = {512,512};
```

```
fbz.range    = {0,100};
```

```

# Display of mask
framebuf fbm {
    string  type,
    short   dispsize[2],
    float   range[2]
};
fbm.type      = "win";
fbm.dispsize  = {512,512};
fbm.range     = {0,255};

# Display of grey value image
framebuf fbg {
    string  type,
    short   dispsize[2],
    float   range[2]
};
fbg.type      = "win";
fbg.dispsize  = {512,512};
fbg.range     = {0,255};

#####
# Other objects
# Declaration of the variables
#####

byte    mask[512][512];
binary  bmask[512][512];
byte    grey[512][512];
float   x[512][512];
float   y[512][512];
float   z[512][512];
float   test[512][512];
float   fmean;
float   fstd;

byte    seq[20][1][512][512];

XYZMG:=46;

#####
# Operators
#####

operator setup();                                     #
    Abw3dProjCommand("~60h");
    Abw3dProjCommand("k08h");
endoperator;

# Measure 1 image, get the results (X, Y, Z, MASK, and GREY),
# display them and save them in the images subdirectory.

operator measure();
    Abw3dMeasure(XYZMG,1);
    x=Abw3dGetX(); fbx=x;
    y=Abw3dGetY(); fby=y;
    z=Abw3dGetZ(); fbz=z;
    mask=Abw3dGetMask();
    bmask=Threshold(mask,{1,255y});

```

```
    fbm=bmask;
    grey=Abw3dGetGrey(); fbg=grey;

    Write("x.tif",x,"replace");
    Write("y.tif",y,"replace");
    Write("z.tif",z,"replace");
    Write("mask.tif",mask,"replace");
    Write("grey.tif",grey,"replace");
endoperator;

# The operator Abw3dInit must be called once,
# before Abw-3d can be used in heurisko.
Abw3dInit(fb);

# The operator Abw3dReadParam initialize Abw-3d and the projector with
# the help of the input files belonging to the ABW software package
# (*.inp) to be initialized.
Abw3dReadParam("c:\abwinput\Abw3d.inp");

# declare operator for the reference measurement
operator out = korrektur(in);
float min;
float kmean;
float kvar;
float th[2];
float korin[512][512];
float hkor[512][512];
float fkor1[512][512];
binary bk[512][512];

kmean=MeanOf(in);
List(kmean);
kvar=VarianceOf(in,kmean);
kvar=Sqrt(kvar);
kvar=Mul(kvar,4.0);
th[0]=Sub(kmean,kvar);
th[1]=Add(kmean,kvar);
bk=Threshold(in,th);
korin=bk;
fkor1=Mul(in,korin);

fb=fkor1;
korin=Mul(korin,-1.0);
korin=Add(korin,1.0);
hkor=kmean;
hkor=Mul(korin,hkor);
korin=Add(fkor1,hkor);
fb=korin;
out=korin;
endoperator;

fbz.range={0.0,450.0}; # Gray tones from 0 to 450
fbz=z;

# calibration operator
operator cal();
float kref[512][512];
Abw3dProjDimm(96);

wait;
```

```
# to warm up the projector
pause("Projector is warming up!");
wait(60);
```

```
#1
pause("0-Cal");
Abw3dCalibrateCapture(0);
Abw3dProjDimm(96);
```

```
#2
pause("75-Cal");
Abw3dCalibrateCapture(75);
Abw3dProjDimm(96);
```

```
#3
pause("150-Cal");
Abw3dCalibrateCapture(150);
Abw3dProjDimm(96);
```

```
#4
pause("225-Cal");
Abw3dCalibrateCapture(225);
Abw3dProjDimm(96);
```

```
#5
pause("300-Cal");
Abw3dCalibrateCapture(300);
Abw3dProjDimm(96);
```

```
#6
pause("375-Cal");
Abw3dCalibrateCapture(375);
Abw3dProjDimm(96);
```

```
#7
pause("495-Cal");
Abw3dCalibrateCapture(495);
Abw3dProjDimm(96);
```

```
#8
pause("595-Cal");
Abw3dCalibrateCapture(595);
Abw3dProjDimm(96);
```

```
#9
pause("695-Cal");
Abw3dCalibrateCapture(695);
Abw3dProjDimm(96);
```

```
#10
pause("795-Cal");
Abw3dCalibrateCapture(795);
Abw3dProjDimm(96);
```

```
#11
pause("895-Cal");
Abw3dCalibrateCapture(895);
Abw3dProjDimm(96);
```

```
#12
```

```

pause("995-Cal");
Abw3dCalibrateCapture(995);
Abw3dProjDimm(96);

Abw3dCalibrate();
string cal;
SetPathW("c:\abwinput");
# save the calibration
Abw3dWriteCal("c:\abwinput\cal");
Abw3dProjDimm(96);

pause("Zero-level base plane measurement");
kref=0.0;
measure();
kref=korrektur(z);
kref=TP-Filter(kref,{4,4});
# save reference to c:\abwinput\ref.tif
Write("ref.tif",kref,"replace");
Abw3dProjDimm(96);
endoperator;

cal(); # start the calibration
SetPathR("c:\abwinput");
x=Read("ref.tif");
fbm=x;

```

11.2 Measurement program

```

# Curl measurement

#####
# Framebuffers
#####

# Framegrabber
# an Object to save Images
framebuf fb {
    string type,
    string config,
    float range[2],
    short live,
    short videoin,
    short sync
};
fb.type = "pc_eye1";
fb.config = "cvm10.dat";
fb.range = {0,255};

# Display of x coordinates
framebuf fbx {
    string type,
    short dispsize[2],
    float range[2]
};

```

```
fbx.type      = "win";
fbx.dispsize  = {512,512};
fbx.range     = {-400,400};
```

```
# Display of y coordinates
```

```
framebuf fby {
    string  type,
    short   dispsize[2],
    float   range[2]
};
fby.type      = "win";
fby.dispsize  = {512,512};
fby.range     = {-400,400};
```

```
# Display of z coordinates
```

```
framebuf fbz {
    string  type,
    short   dispsize[2],
    float   range[2]
};
fbz.type      = "win";
fbz.dispsize  = {512,512};
fbz.range     = {0,250};
```

```
# Display of mask
```

```
framebuf fbm {
    string  type,
    short   dispsize[2],
    float   range[2]
};
fbm.type      = "win";
fbm.dispsize  = {512,512};
fbm.range     = {0,255};
```

```
# Display of grey value image
```

```
framebuf fbg {
    string  type,
    short   dispsize[2],
    float   range[2]
};
fbg.type      = "win";
fbg.dispsize  = {512,512};
fbg.range     = {0,255};
```

```
#####
```

```
# Other objects
```

```
# Declaration of the variables
```

```
#####
```

```
byte   mask[512][512];
binary bmask[512][512];
byte   grey[512][512];
float  x[512][512];
float  y[512][512];
float  z[512][512];
float  fmean;
float  fstd;
float  ref[512][512];
byte   seq[20][1][512][512];
```

```

XYZMG:=46;

float korm[512][512];
float test[512][512];
float ferg[4];
float erg[4][200];

string datekonf;

#####
# Operators
#####

operator setup();
    Abw3dProjCommand("~60h");
    Abw3dProjCommand("k08h");
endoperator;

# Measure 1 image, get the results (X, Y, Z, MASK, and GREY),
# display them and save them in the images subdirectory.
operator measure();
    Abw3dProjDimm(96);
    Abw3dMeasure(XYZMG,1);
    x=Abw3dGetX(); fbx=x;
    y=Abw3dGetY(); fby=y;
    z=Abw3dGetZ(); fbz=z;
    mask=Abw3dGetMask();
    bmask=Threshold(mask,{1,255y});
    fbm=bmask;
    grey=Abw3dGetGrey();
    fbg=grey;
    Abw3dProjDimm(0);
endoperator;

# The operator Abw3dInit must be called once,
# before Abw-3d can be used in heurisko.
Abw3dInit(fb);

# The operator Abw3dReadParam initialize Abw-3d and the projector with
# the help of the input files belonging to the ABW software package
# (*.inp) to be initialized.
Abw3dReadParam("c:\abwininput\Abw3d.inp");

# Read in the zero-level base plane.
SetPathR("c:\abwininput");
ref=Read("ref.tif");

# Read in the calibration values
string cal;
Abw3dReadCal("c:\abwininput\cal");

operator eout = hoehen(in);      #eout = output of results
    float xmean;
    float var;
    float min;
    float max;

```

```

float fout[512][512];

fout = TP-Filter(in, {256, 256}); # Low-pass filter over original
image ('in')
xmean = MeanOf(fout);           # Calculation average value
fout = Sub(fout, xmean);        # subtraction fout - xmean
fout = Sub( in, fout);
fout =Mul(fout,10.0);           # multiplication fout * 10 (µm)
xmean=MeanOf(fout);            # Average value corrected image
fb=fout;

var = VarianceOf(fout,xmean);   # variance
var = Sqrt(var);                # standard deviation
max = MaxOf(fout);              # Max value
min = MinOf(fout);             # Min value
eout[0]=xmean;
eout[1]=var;
eout[2]=min;
eout[3]=max;
endoperator;

fbz.range={0.0,250.0};          # display 250 gray tones
fbz=z;
short sn;
short nr;

string sname;
nr=1;
SetFormat(nr,"%0d");

#T.Mikova
#operator for waiting period between two measurements
#w is the time in Sec
operator waitzwMessungen(w);
    wait;
    wait(w);
endoperator;

#Abw3dProjDimm(96);
Abw3dProjDimm(0);
#Abw3dProjDimm(146);

#T.Mikova
#declaration of the variables
string filenameX;
string filenameY;
string filenameZ;
string filenameM;
string filenameG;
string filenameERG;
string filenameGREY;
string filenameTEST;
string strnr;

operator loop();                # Actual measuring routine

short live;
byte btest[512][512];

```

```
#declaration of the variables
#and controlling of the inputs windows (Messageboxs)

short waitsek;
short anzahlmessungen;
short dienull;

waitsek=Input("Please enter the time between two measurements in
seconds:");
anzahlmessungen=Input("Please enter the number of measurements:");

dienull=0;

if (waitsek==dienull);
    waitsek=2;
endif;

if (anzahlmessungen==dienull);
    anzahlmessungen=1;
endif;

if (anzahlmessungen>dienull);

    pause("Put in your sample!");

    repeat(anzahlmessungen);
        live=fb.live;
        fb.live=-1;

        measure();
        #Abw3dProjDimm(96);
        Abw3dProjDimm(0);
        #Abw3dProjDimm(146);

        test=z;
        fb=z;
        fbm=bmask;
        test=Sub(test,ref);      #Subtraction of the reference level
        fbz=test;
        ferg=hoehen(test);      #measure of the image statistics,
average value, min, max

        erg[0][nr]=ferg[0];
        erg[1][nr]=ferg[1];
        erg[2][nr]=ferg[2];
        erg[3][nr]=ferg[3];

        # write the results to files
        SetPathW("c:\Tmp\testMikova");

        strnr=nr;
        strnr=Add(strnr, ".asc");
        filenameX=Add("x_", strnr);
        filenameY=Add("y_", strnr);
        filenameTEST=Add("test_", strnr);

        #Write plain ASCII image
        Write(filenameX,x);
```

```

Write(filenameY,y);
Write(filenameTEST,test);

strnr=nr;
strnr=Add(strnr, ".tif");
filenameGREY=Add("grey_",strnr);

#Write TIFF image
Write(filenameGREY,greyscale,"replace");

if (nr<anzahlmessungen);
    waitzwMessungen(waitsek);
    nr=Add(nr,1);
endif;

endrepeat;

Write("TimeIntv.asc",waitsek); # time interval between two
measurements.

fb.live=live;
else;
    pause("The measurement cannot be started. Please restart the
program!");
endif;
endoperator;

loop();

```

11.3 Analysis program

```

function curl_analysis

% Curl Analysis for AiF project 14169N
% 2004-2006, Shulei Zhao, PMV, TU-Darmstadt.
close all, clear all
%
h_fg = figure(...
    'BackingStore', 'off',...
    'IntegerHandle', 'off',...
    'MenuBar', 'none',...
    'Name', 'Curl Analysis',...
    'NumberTitle', 'off',...
    'Position', [50,50,700,560],...
    'Resize', 'off',...
    'Tag', 'Curl_fig',...
    'ToolBar', 'none',...
    'Units', 'pixels');
%
h_panell = uipanel(...
    'Parent', h_fg,...
    'Position', [0,0,0.8,1],...
    'Tag', 'imPanel');
%
IM_ = load('IM_curl.mat'); curl_a = IM_.curl_a; curl_c = IM_.curl_c;
h_im = image(curl_a);

```

```

set(h_im, 'Alphadata', curl_c,...
          'Clipping', 'off',...
          'Tag', 'Curl_image');
set(gca, 'Position', [109,86,344,389]/560,...
        'Parent', h_panell,...
        'Visible', 'off');

%
uicontrol(...
    'HorizontalAlignment', 'left',...
    'Parent', h_panell,...
    'Position', [33 538 500 15],...
    'String', '',...
    'Style', 'text',...
    'Tag', 'imPathInfo');

uicontrol(...
    'Visible', 'off',...
    'HorizontalAlignment', 'left',...
    'Parent', h_panell,...
    'Position', [133 3 50 15],...
    'String', 'Pixel info:',...
    'Style', 'text',...
    'Tag', 'imPixInfo1');

uicontrol(...
    'Visible', 'off',...
    'HorizontalAlignment', 'left',...
    'Parent', h_panell,...
    'Position', [181 3 81 15],...
    'String', '(X, Y) Intensity',...
    'Style', 'text',...
    'Tag', 'imPixInfo2');

h_panel = uipanel('Parent',h_fg,'Position',[0.8,0,0.2,1]);
h_push1 = uicontrol(...
    'Callback', @push1_load,...
    'Position', [20,500,100,30],...
    'Parent', h_panel,...
    'SelectionHighlight', 'off',...
    'FontWeight', 'bold',...
    'String', 'Load Image',...
    'Style', 'pushbutton',...
    'Tag', 'push_1',...
    'TooltipString', 'Load an image contains curl.');
```

```

h_push2 = uicontrol(...
    'Callback', @push2_analysis,...
    'Enable', 'off',...
    'Position', [20,450,100,30],...
    'Parent', h_panel,...
    'SelectionHighlight', 'off',...
    'FontWeight', 'bold',...
    'String', 'Analyze',...
    'Style', 'pushbutton',...
    'Tag', 'push_2',...
    'TooltipString', 'Analyse the selected areas.');
```

```

h_push3 = uicontrol(...
    'Callback', 'closereq',...
    'Position', [20,400,100,30],...
    'Parent', h_panel,...

```

```

        'SelectionHighlight',    'off',...
        'FontWeight',          'bold',...
        'String',              'Exit',...
        'Style',                'pushbutton',...
        'Tag',                  'push_3',...
        'TooltipString',        'Exit the program. ');

% sub-functions

function push1_load(varargin)
% load image and display it in left panel.
persistent lastDir

if isempty(lastDir)
    [FileName,PathName,FilterIndex_1] = uigetfile('*.tif',...
        'Please select all TIF file that you want to analyse...',...
        'MultiSelect','on');
else
    [FileName,PathName,FilterIndex_1] = uigetfile('*.tif',...
        'Please select all TIF file that you want to analyse...',...
        lastDir,'MultiSelect','on');
end

if FilterIndex_1 == 1% only 'tif' files are allowed to be selected
    lastDir = PathName;
    if iscell(FileName) % when multi files are selected.
        N_FileSelected = length(FileName); % number of files been selected.
        temp = [];
        for i = 1:N_FileSelected
            temp(i) = str2num(number_in_file_name(FileName{i}));
        end
        [B,Ix] = sort(temp);
        FileName = FileName(Ix);

        I = imread([PathName,FileName{end}]);
        set(findobj('Tag','imPathInfo'),'String',[PathName,FileName{end}]);
    else % only one file is selected.
        B = str2num(number_in_file_name(FileName));
        I = imread([PathName,FileName]);
        set(findobj('Tag','imPathInfo'),'String',[PathName,FileName]);
    end

    delete(findobj('Tag','Curl_image'));
    h = imshow(I);
    set(gca,'Position',[24,24,512,512]/560);
    set(findobj('Tag','Curl_fig'),...
        'WindowButtonMotionFcn', @my_cursor_move,...
        'KeyPressFcn', @rect_delete);
    set(h,'ButtonDownFcn',@buttonDownOverImage,'Tag','Curl_image');
    set(findobj('Tag','imPixInfo1'),'Visible','on');
    set(findobj('Tag','imPixInfo2'),'Visible','on');
    set(findobj('Tag','imPathInfo'),'Visible','on');
    setappdata(findobj('Tag','Curl_fig'),'PathName',PathName);
    setappdata(findobj('Tag','Curl_fig'),'NumFiles',B);
end
end % end of function push1_load

function push2_analysis(varargin)
% analyse the selected areas.
h = findobj('Type','rectangle');
if ~isempty(h)

```

```

h_1 = findobj(gca,'Type','line'); delete(h_1);
htxt = findobj(gca,'Type','text'); delete(htxt);
excelName = datestr(now,'mmmddyHHMM');
B = getappdata(findobj('Tag','Curl_fig'),'NumFiles');
PathName = getappdata(findobj('Tag','Curl_fig'),'PathName');

rects = zeros(length(h),4);
for ii = 1:1 % only one area is allowed.
    rects(ii,:) = get(h(ii),'Position');
end

for ii = 1:length(B) % number of image files.
    fid = zeros(3,1);
    fid(1) = fopen([PathName,'x_',num2str(B(ii)),'.asc'],'r');
    if fid(1) == -1
        disp([PathName,'x_',num2str(B(ii)),'.asc file CANNOT BE
OPEN!']);
    else
        X = fscanf(fid(1),'%f',[512,512]);
        fclose(fid(1));
    end

    fid(2) = fopen([PathName,'y_',num2str(B(ii)),'.asc'],'r');
    if fid(2) == -1
        disp([PathName,'y_',num2str(B(ii)),'.asc file CANNOT BE
OPEN!']);
    else
        Y = fscanf(fid(2),'%f',[512,512]);
        fclose(fid(2));
    end

    fid(3) = fopen([PathName,'test_',num2str(B(ii)),'.asc'],'r');
    if fid(3) == -1
        disp([PathName,'test_',num2str(B(ii)),'.asc file CANNOT BE
OPEN!']);
    else
        Z = fscanf(fid(3),'%f',[512,512]);
        fclose(fid(3));
    end

    if any(fid == -1)
        % do not analyse.
    else
        for jj = 1:length(h) % selected areas.

            xjj = X(rects(jj,1):rects(jj,1)+rects(jj,3),...
                rects(jj,2):rects(jj,2)+rects(jj,4));
            yjj = Y(rects(jj,1):rects(jj,1)+rects(jj,3),...
                rects(jj,2):rects(jj,2)+rects(jj,4));
            zjj = Z(rects(jj,1):rects(jj,1)+rects(jj,3),...
                rects(jj,2):rects(jj,2)+rects(jj,4));
            Ra{ii} = star_curl(xjj,yjj,zjj,rects(jj,:));

        end

        % get file information
        f_info = dir([PathName,'test_',num2str(B(ii)),'.asc']);

        % write results to excel file.
        results_file = fullfile(PathName,[excelName,'.xls']);
        % header.....
        xlswrite(results_file, {[PathName,'*_ ',num2str(B(ii)),...
            '.asc']}, ii, 'A1');
        xlswrite(results_file,{datestr(f_info.date,1),...

```

```

        datestr(f_info.date,13)},ii,'L1:M1');

titles_1 = {'Area No.','Curl Radii (mm)','Curl Radii Std
(mm)',...
           'Curl Height (mm)','Curvature (1/m)'};
xlswrite(results_file,titles_1(1),ii,'A2');
xlswrite(results_file,titles_1(2),ii,'B2');
xlswrite(results_file,titles_1(3),ii,'E2');
xlswrite(results_file,titles_1(4),ii,'H2');
xlswrite(results_file,titles_1(5),ii,'K2');
titles_2 = {'CD','MD','Diagonal','CD','MD','Diagonal',...
           'CD','MD','Diagonal','CD','MD','Diagonal'};
xlswrite(results_file,titles_2,ii,'B3');
% .....
xlswrite(results_file,round([Ra{ii}(:,1:10),...
    1000./Ra{ii}(:,2:4)]*100)/100,ii,'A4');
progressbar(ii/length(B),4)
    end
end
end
end % end of sub function push2_analysis

function my_cursor_move(varargin)
% show image information at cursor location.
h1 = findobj('Tag','Curl_fig'); % figure
h2 = findobj('Tag','Curl_image'); % image
h3 = get(h2,'Parent'); % axis
new_point = get(h3,'CurrentPoint');
h4 = findobj('Tag','imPixInfo2'); % text

if any(new_point(1,1:2)<0.5) || any(new_point(1,1:2)>512)% outside of image
    set(h1,'Pointer','arrow')
    set(h4,'String','(X, Y) Intensity');
else
    Cdata = get(h2,'CData');
    set(h1,'Pointer','fullcrosshair'), %fullcrosshair
    ColorIntensity = Cdata(round(new_point(1,2)),round(new_point(1,1)));
    XYCstring = sprintf('(%1.0f, %1.0f) %1.0f',new_point(1,1:2), ...
        ColorIntensity);
    set(h4,'String',XYCstring);
end
end % end of sub fun my_cursor_move

function buttonDownOverImage(varargin)
% mouse button is pressed over an image.
h = findobj(gca,'Type','Line');
point = get(gca,'CurrentPoint');

if isempty(h)
    point1 = point(1,1:2);
    hold on,
    line([0 512],[point1(2),point1(2)],'Color',[1,0,0],'LineStyle','--'),
    line([point1(1),point1(1)],[0 512],'Color',[1,0,0],'LineStyle','--'),
    hold off; drawnow;
    setappdata(findobj('Tag','Curl_fig'),'ud_point',point1(1,1:2));
else
    delete(h)
    point2= point(1,1:2);
    if point2(1)>512
        point2(1) = 512;
    elseif point2(1)<1

```

```

        point2(1)=1;
    end

    if point2(2)>512
        point2(2) = 512;
    elseif point2(2)<1
        point2(2)=1;
    end

    point1 = getappdata(findobj('Tag','Curl_fig'),'ud_point');
    points = [point1; point2];
    rect = round([min(points),max(points)-min(points)]);
    if any(rect(3:4)<20) || max(rect(3:4))<50
        % selected area is too small, update point.
        hold on,
        line([0 512],[point2(2),point2(2)],'Color',[1,0,0],'LineStyle','--
    '),
        line([point2(1),point2(1)],[0 512],'Color',[1,0,0],'LineStyle','--
    '),
        hold off; drawnow;
        setappdata(findobj('Tag','Curl_fig'),'ud_point',point2(1,1:2));
    else
        hold on,
        h=rectangle('Position',rect,'LineWidth',3,'EdgeColor','b');
        hold off
        set(h,'ButtonDownFcn',@rect_selection);
        set(findobj('Tag','push_2'),'Enable','on');
    end
end
end

end % end of fub fun buttonDownOverImage

function rect_selection(varargin)
% highlight the selected rectangle.
switch get(varargin{1},'Selected')
    case 'on'
        set(varargin{1},'EdgeColor','b','Selected','off'),
    otherwise
        set(varargin{1},'EdgeColor','r','Selected','on'),
end
drawnow,
end % end of sub function rect_selection

function rect_delete(varargin)
% delete the selected rectangle.
switch varargin{2}.Key
    case 'delete'
        h = findobj(gca,'Type','Line');
        delete(h)
        h=findobj('Type','rectangle','Selected','on');
        delete(h)
        if isempty(findobj('Type','rectangle'))
            set(findobj('Tag','push_2'),'Enable','off');
        end
    end
end
end % end of sub function rect_delete

end % end of curl_analysis

```

```

function Ra = star_curl(xjj,yjj,zjj,rects)
% called by curl_analysis
% 2004-2006, Shulei Zhao, PMV, TU-Darmstadt.

% close figures except the main GUI.
h_figs = get(0,'Children');
h1     = findobj('Tag','Curl_fig');% main figure
h2     = findobj('Tag','ProgressBar');
h_figs = setdiff(h_figs,[h1,h2]);
close(h_figs)

cc = 0.3; % the variation of the metal plate. [mm]
% divide the image intor 8 sub-areas.
% o -----> dy
% |
% |           m2
% |      c1/-----\c2
% |     /            \
% |    c8/            \c3
% |   /              \
% |  m5              m3
% | /                \
% |c7\              /c4
% | \                /
% |  c6\-----/c5
% |           m4
% |
% v
% dx

m_p = zeros(5,2); % middle points, m1 - m5.

zjj = zjj/100; % mm.
[mm,nn]=size(zjj);
m_p(1,:) = [floor(mm/2),floor(nn/2)];
% initial guess.

% plot the position on main image.
figure(h1),hold on,
plot(rects(1)+m_p(1,1),rects(2)+m_p(1,2),'b.'), hold off

z_center = mean(mean(zjj(m_p(1,1)-10:m_p(1,1)+10,m_p(1,2)-10:m_p(1,2)+10)));

% center covered with a meatal.

% locate the meatal plate.

zf = comput_molecules(zjj);

% vertical direction.
pp = mp_search(zf(:,m_p(1,2)),m_p(1,1),cc);
m_p(2,1) = pp(1);
m_p(4,1) = pp(2);

% horizontal direction.
pp = mp_search(zf(m_p(1,1),:),m_p(1,2),cc);
m_p(5,2) = pp(1);
m_p(3,2) = pp(2);

```

```

% reset mp
m_p(1,1) = round(mean([m_p(2,1),m_p(4,1)]));
m_p(1,2) = round(mean([m_p(5,2),m_p(3,2)]));
pp = mp_search(zf(:,m_p(1,2)),m_p(1,1),cc);
m_p(2,1) = pp(1); m_p(2,2) = m_p(1,2);
m_p(4,1) = pp(2); m_p(4,2) = m_p(1,2);
pp = mp_search(zf(m_p(1,1,:),m_p(1,2),cc);
m_p(5,2) = pp(1); m_p(5,1) = m_p(1,1);
m_p(3,2) = pp(2); m_p(3,1) = m_p(1,1);

% plot the new position on main image.
figure(h1),hold on,
plot(rects(1)+m_p(1,1),rects(2)+m_p(1,2),'m. '), hold off

if z_center > 0.5
% search for corner points
c_p = cp_search(zf,m_p,cc);
else
[x,y] = getpts(gca);
c_p(:,1) = round(x)-rects(1);
c_p(:,2) = round(y)-rects(2);
end

% display the misalignment of the metal object.
disp([num2str([atan((c_p(1,1)-c_p(2,1))/(c_p(2,2)-c_p(1,2)))/pi*180, ...
atan((c_p(4,2)-c_p(3,2))/(c_p(4,1)-c_p(3,1)))/pi*180, ...
atan((c_p(5,1)-c_p(6,1))/(c_p(6,2)-c_p(5,2)))/pi*180, ...
atan((c_p(7,2)-c_p(8,2))/(c_p(7,1)-c_p(8,1)))/pi*180]),' °C'])

% outline the metal object.
figure(h1),hold on,
line(rects(1)+c_p([8,1,2,3,4,5,6,7,8],1),rects(2)+...
c_p([8,1,2,3,4,5,6,7,8],2),'Color','m'),
hold off

% calculate dx, dy, use measurement data over the metal plate.
p(1) = max(c_p([3,8],1)); % row start
p(2) = min(c_p([7,4],1)); % row end
p(3) = max(c_p([1,6],2)); % column start
p(4) = max(c_p([2,5],2)); % column end

xi = xjj(p(1):p(2),p(3):p(4));
dx = mean(diff(mean(xi,2)));

yi = yjj(p(1):p(2),p(3):p(4));
dy = mean(diff(mean(yi,1)));

ap = [1, c_p(8,1), 1, c_p(1,2) % area1
1, min(c_p([1,2],1))-2, c_p(1,2), c_p(2,2) % area2
1, c_p(3,1), c_p(2,2), nn-2 % area3
c_p(3,1), c_p(4,1), max(c_p([3,4],2))+2, nn-2 % area4
c_p(4,1), mm-2, c_p(5,2), nn-2 % area5
max(c_p([5,6],1))+2, mm-2, c_p(6,2), c_p(5,2) % area6
c_p(7,1), mm-2, 1, c_p(6,2) % area7
c_p(8,1), c_p(7,1), 1, min(c_p([7,8],2))-2]; % area8

% plot the sub-areas
figure(h1),hold on,

```

```

for i = 1:8
    line(rects(1)+[ap(i,1),ap(i,1),ap(i,2),ap(i,2),ap(i,1)],...
         rects(2)+[ap(i,3),ap(i,4),ap(i,4),ap(i,3),ap(i,3)], 'Color', 'g'),
        text(rects(1)+ap(i,1)+15,rects(2)+ap(i,3)+15,num2str(i), 'Color', 'g'),
end
hold off

Ra = [];
for i = 1:1:8
    A = zjj(ap(i,1):ap(i,2),ap(i,3):ap(i,4));
    A(A<0)=0;
    Rat = curl_of_sub_area(A,dx,dy,i);
    Ra = [Ra;i*ones(size(Rat,1),1),Rat];
end

% display the curl in star shape sample as true color image.
zjj(zjj<0) = NaN;
figure(22),clf,surf(zjj,'EdgeColor','interp'),
h_cb=colorbar; view(90,90),
ylabel('Machine Direction'),xlabel('Cross-Machine Direction')
title('Paper Curl'),set(gca,'XTickLabel',[],'YTickLabel',[])
cb_tick = get(h_cb,'YTickLabel');
for iii = 1:length(cb_tick)
    cb_tick1{iii} = [cb_tick(iii),'mm'];
end
set(h_cb,'YTickLabel',cb_tick1)

```

```

function zf = comput_molecules(z)
% this function use computational molecules to smooth 2-dimentional data.
% z input data with noise,
% zf filtered data.

mask = [1,2,1;2,12,2;1,2,1]./24;
zf = conv2(z,mask);
zf([1,end],:) = []; % remove edge.
zf(:,[1,end]) = [];

```

```
function [xc,yc,R,a] = circfit(x,y)
% fits a circle in x,y plane.
% x,y are column vector where (x(i),y(i)) is a measured point.
%
% result is center point (yc,xc) and radius R.
% an optional output is the vector of coefficient a
% describing the circle's equation
%  $x^2+y^2+a(1)*x+a(2)*y+a(3)=0$ 
x = reshape(x,[],1);
y = reshape(y,[],1);
a = [x, y, ones(size(x))]\[-(x.^2+y.^2)];
xc = -.5*a(1);
yc = -.5*a(2);
R = sqrt((a(1)^2+a(2)^2)/4-a(3));
```